Mathematical Models and Methods for Noninvasive Bioimpedance Imaging

Jin Keun Seo

Computational Science & Engineering
Yonsei University, Korea

ICIAM 2015 at Beijing (2015.8.13)

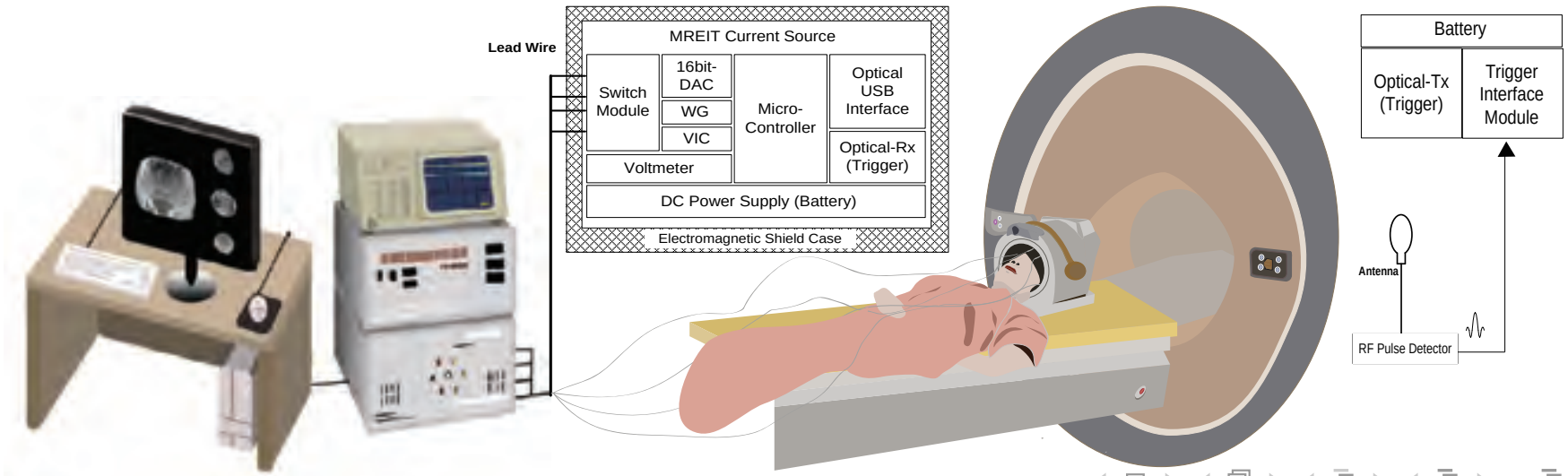

Electrical Tissue Properties Imaging

Aim: Visualize conductivity (σ) and permittivity (ϵ) distribution.

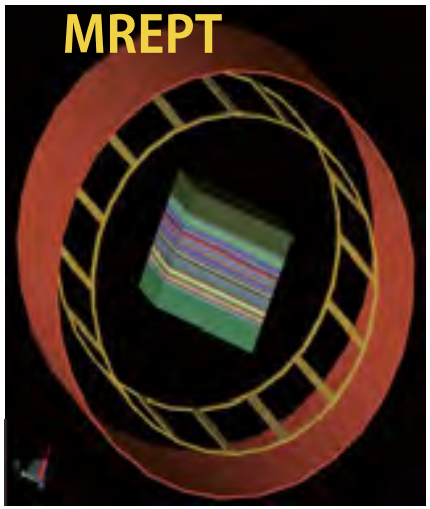

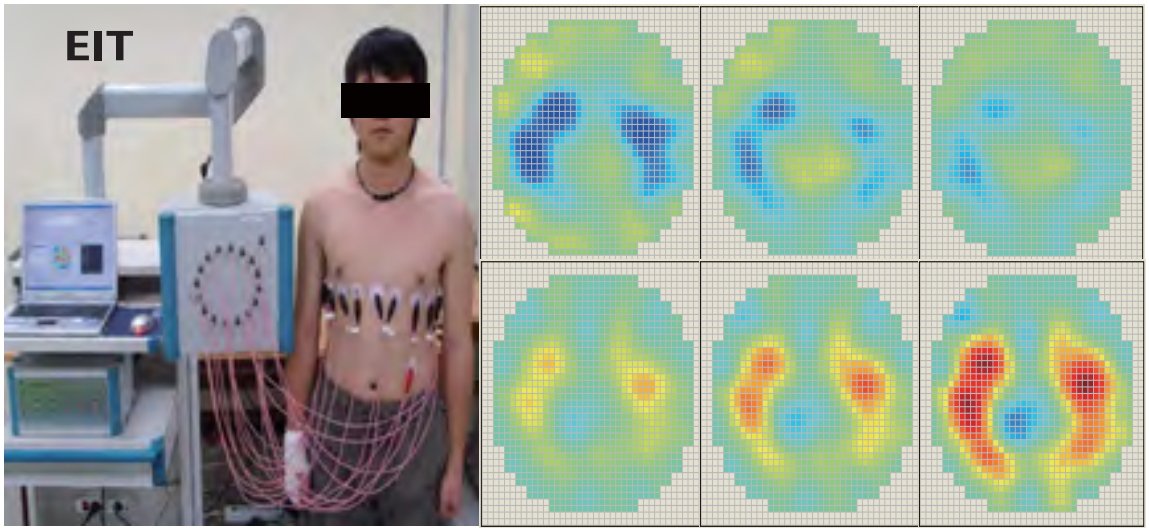

[Seo/Woo, "Magnetic Resonance Electrical Impedance Tomography", SIAM Review, (2011)]

Image Reconstruction of σ (conductivity) / ϵ (permittivity)

Goal: Develop a well-posed system

$$\mathbf{S}\ X \quad = \quad \mathbf{b} \qquad \text{subject to constraints on } X$$

- $X = \sigma, \epsilon$ to be imaged.
- $\mathbf{b}$: Measured data **(boundary current-voltage using electrodes, magnetic field using MRI scanner ...)**
- $\mathbf{S}$: Sensitivity matrix **made from Maxwell equations, data collection method, domain geometry ...**

Major issue: How to convert the ill-posed problem to a well-posed one?

Reconstruction of σ (conductivity) / ϵ (permittivity)

To evaluate them, we must produce **electrical current density J & electric field E** inside the imaging domain Ω.

Inject current (dc / ac)

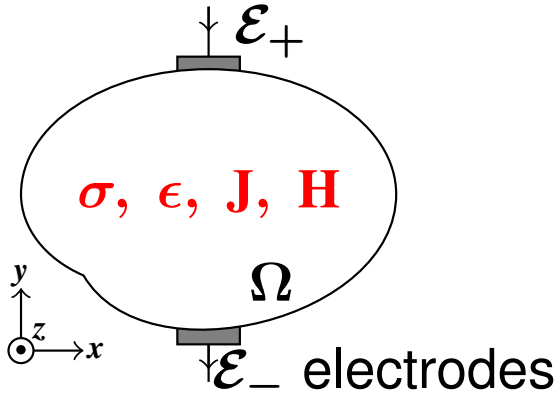

Induce current (ac only)

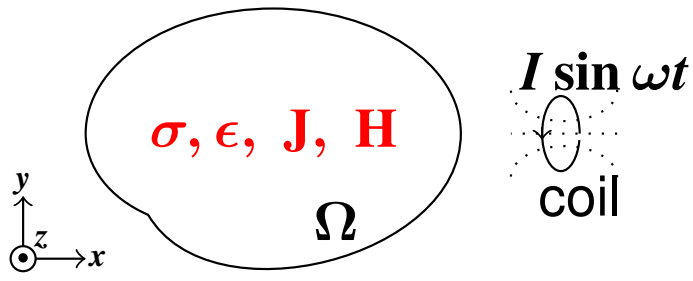

$$\nabla \cdot (\gamma \nabla u) = 0$$

$$-\nabla^2 \mathbf{H} = \nabla \ln \gamma \times \nabla \times \mathbf{H} - i\mu_0 \omega \gamma \mathbf{H}$$

- $\mathbf{E} \approx -\nabla u$ (u :=electric potential), $\mathbf{H}$ (magnetic field), $\gamma = \sigma + i\omega\epsilon$ (admittivity)
- Using this with measurable data, we develop a system $SX = b$.

Electrical conductivity σ & permittivity ϵ

- Electrical tissue properties include **electrical conductivity σ & electrical permittivity ϵ.**

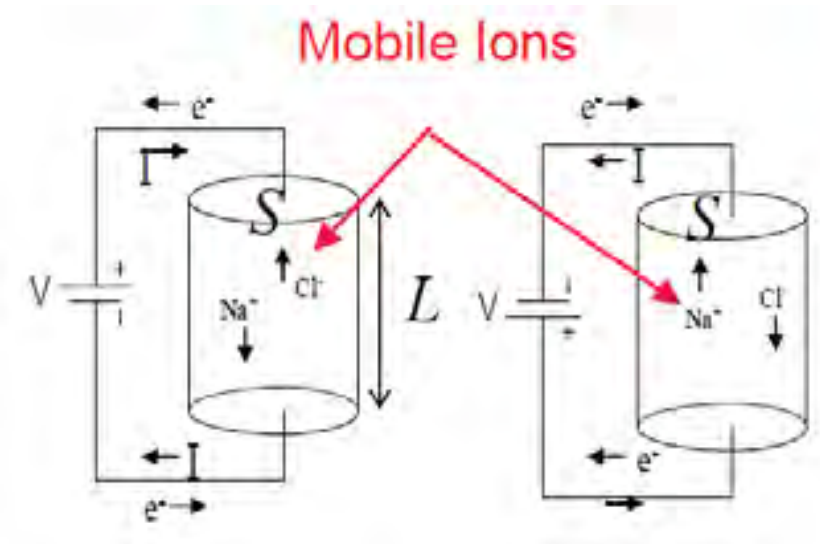

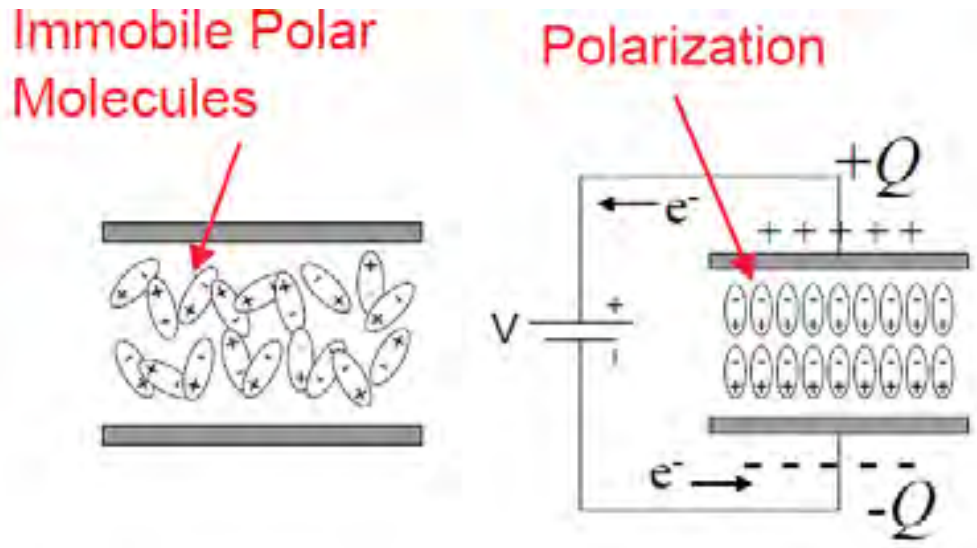

$$\mathbf{J} = \sigma\,\mathbf{E}$$

$$\mathbf{J} = i\omega\epsilon\,\mathbf{E}$$

Cell Structure in Tissues & Effective $\gamma = \sigma + i\omega\epsilon$

$\gamma = \sigma + i\omega\epsilon$ of a biological tissue under the influence of a time-harmonic electric field $\mathbf{E}$ at ω, is determined by its ion concentrations in extra- and intracellular fluids, membrane characteristics and other factors.

$$\int_{Voxel} \mathbf{J} = (\sigma + i\omega\epsilon) \int_{Voxel} \mathbf{E}$$

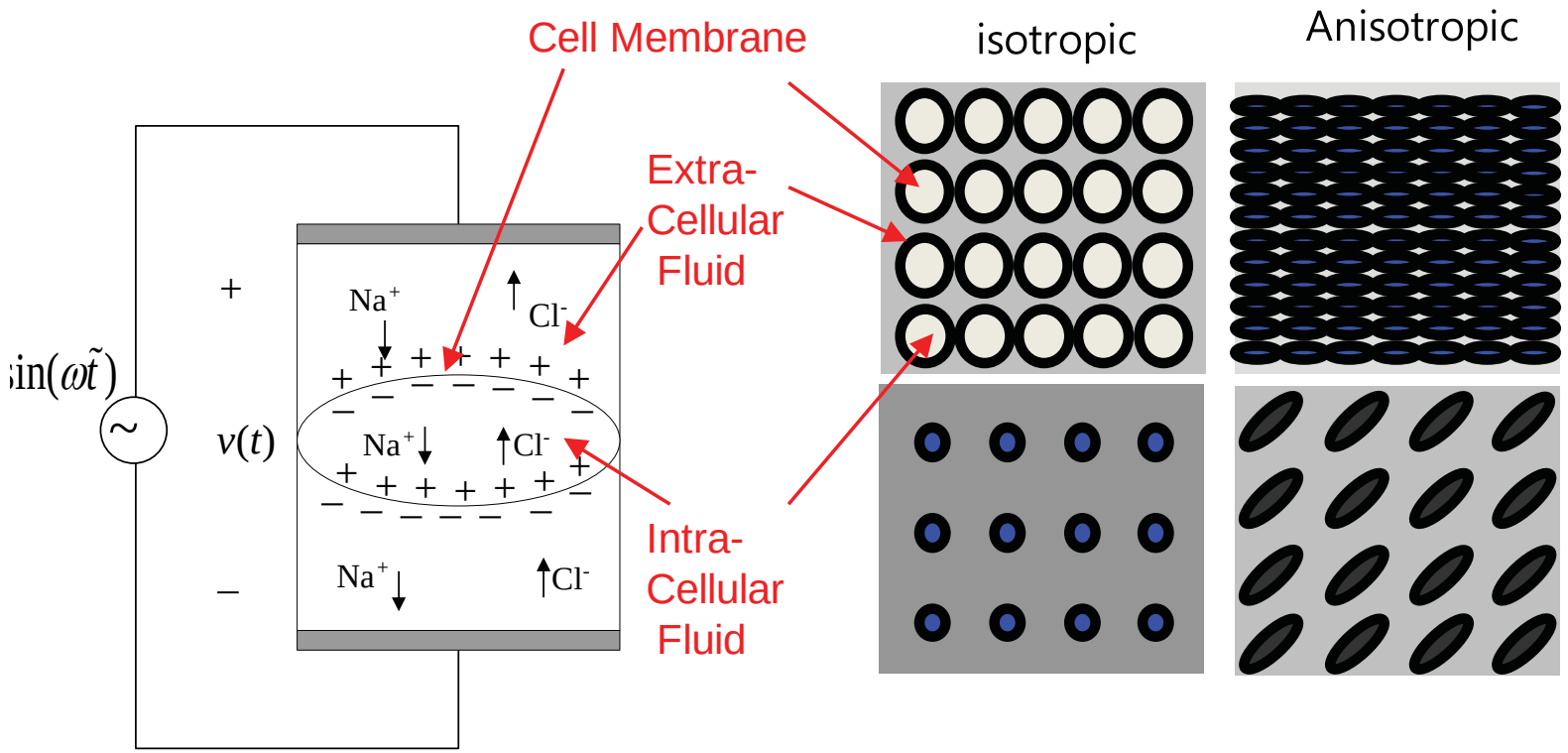

Electrical Tissue Property Imaging

Biological tissues and organs exhibit distinct electrical properties depending on their physiological functions and pathological states

- **Low frequency (0 Hz $\leq \omega/2\pi \leq$ 1MHz):**

$$\nabla \cdot (\underbrace{(\sigma + i\omega\epsilon)}_{\text{conductivity} + i\omega \text{permittivity}} \nabla u) = 0$$

- **Frequency (10 MHz $\leq \omega/2\pi \leq$ 1GHz):**

$$-\nabla^2 \mathbf{H} = \frac{\nabla(\sigma + i\omega\epsilon)}{\sigma + i\omega\epsilon} \times \nabla \times \mathbf{H} - i\mu_0\omega(\sigma + i\omega\epsilon)\mathbf{H}$$

About Data. What is measurable?

Inject current (dc / ac)

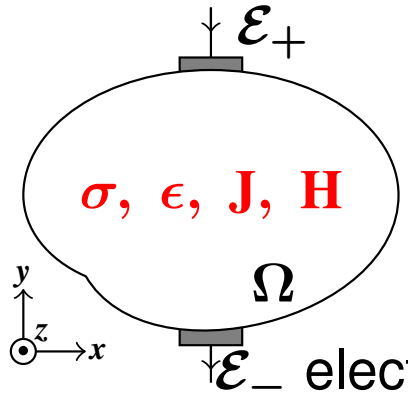

Induce current (ac only)

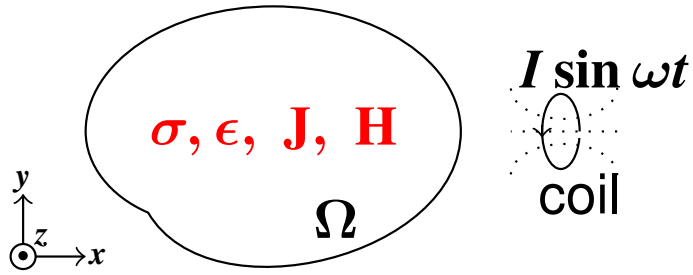

$$\nabla \cdot (\gamma \nabla u) \approx 0 \quad \& \quad -\nabla^2 \mathbf{H} = \nabla \ln \gamma \times (\nabla \times \mathbf{H}) - i\omega\mu\gamma\mathbf{H}$$

- **EIT** ($\leq 1MHz$): Boundary voltage $u|_{\partial\Omega}$ using electrodes.
- **MREIT** ($\leq 1kHz$): Internal H_z using MRI
- **MIT** ($\leq 10MHz$): External magnetic field using coils
- **MREPT** ($128MHz$ at 3T MRI): Internal $H^+ = \frac{1}{2}(H_x + iH_y)$

Compute σ using $\nabla u \parallel (0,0,1)$

To compute σ of a cylindrical object Ω by Ohm's law, we inject a DC current of ImA between top and bottom surface electrodes, and measure the voltage difference V between the electrodes.

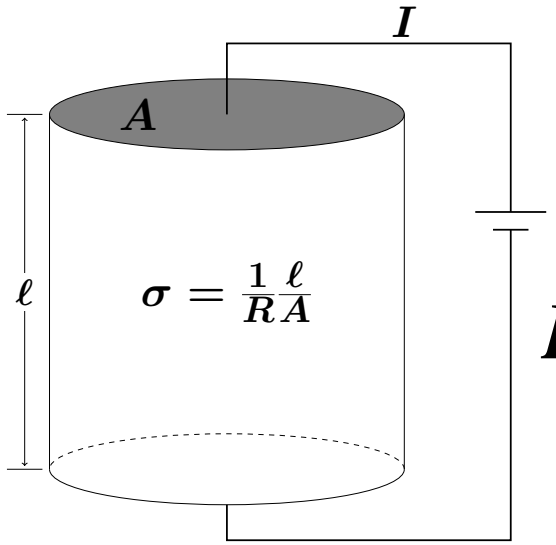

$$\sigma = \frac{1}{R}\frac{l}{A}, \quad V = IR$$

R : resistance of the cylinder

A : electrode surface area

l : length

Here, V is $V = u|_{\text{top}} - u|_{\text{bottom}}$, where u is the potential generated by the injection current:

$$\begin{cases} \nabla \cdot (\sigma \nabla u) &= 0 \quad \text{in } \Omega \\ \sigma \frac{\partial u}{\partial \nu}\Big|_{\partial\Omega} &= \frac{I(mA)}{A(area)} \left(\chi_{\text{top}} - \chi_{\text{bottom}}\right) \end{cases}$$

Compute $\sigma + i\omega\epsilon$ using $\nabla u \parallel (0,0,1)$

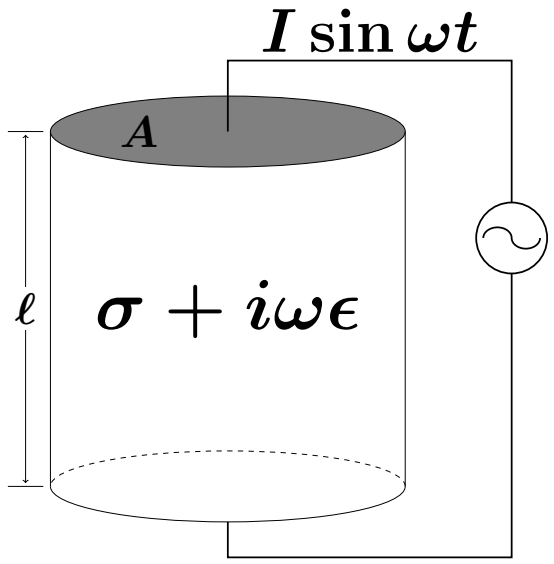

The admittivity γ is computed by

$$\gamma = \sigma + i\omega\epsilon = \frac{1}{Z}\frac{\ell}{A}$$

- $Z = V/I$: impedance.
- ϵ permittivity

$V = u|_{\text{top}} - u|_{\text{bottom}}$ where u satifies

$$\begin{cases} \nabla \cdot (\gamma \nabla u) = 0 \quad \text{in } \Omega \\ \gamma \frac{\partial u}{\partial \nu}\big|_{\partial\Omega} = I/A \left(\chi_{\text{top}} - \chi_{\text{bottom}}\right) \end{cases}$$

How to measure γ for non-cylindrical domain Ω?

We cannot control ∇u unlike CT & MRI! It is determined by the geometry Ω & the current driving electrodes (P_1^+, P_1^-).

$$\nabla \cdot (\gamma \nabla u^1) = 0 \text{ in } \Omega, \quad \gamma \frac{\partial u^1}{\partial \nu}|_{\partial\Omega} = I[\delta(P_1^+ - \cdot) - \delta(P_1^- - \cdot)]$$

$\gamma = ??$

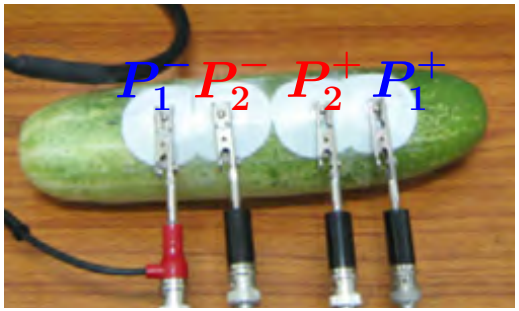

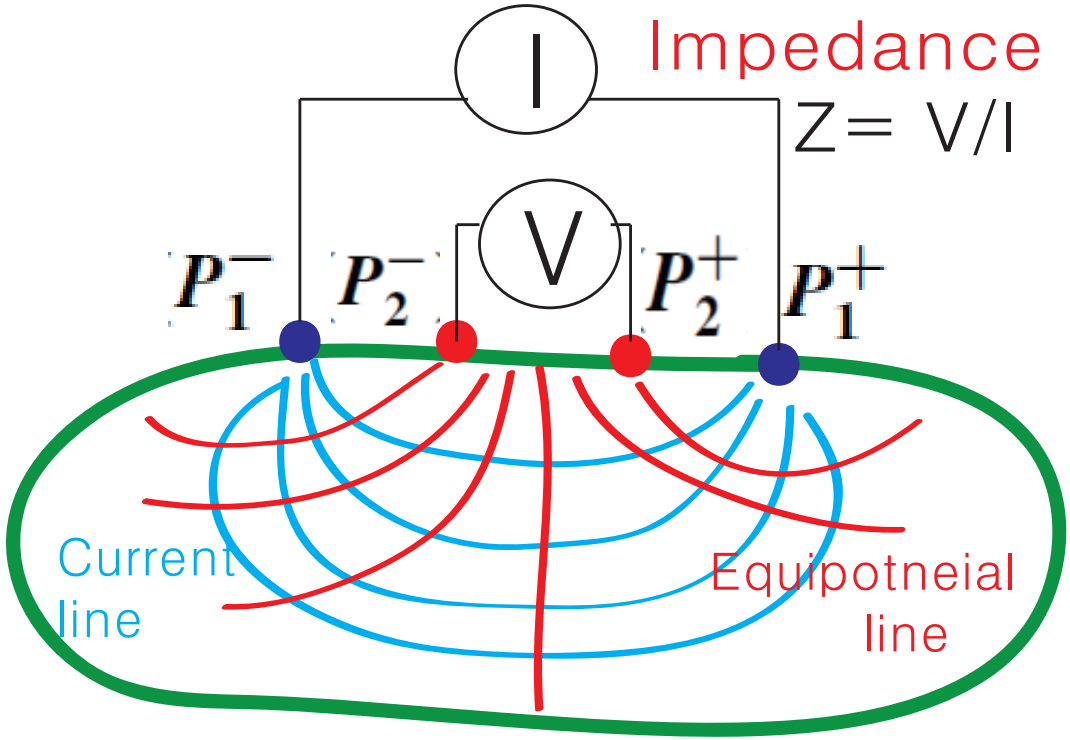

Math. Formula for Computing $\gamma = \sigma + i\omega\epsilon$

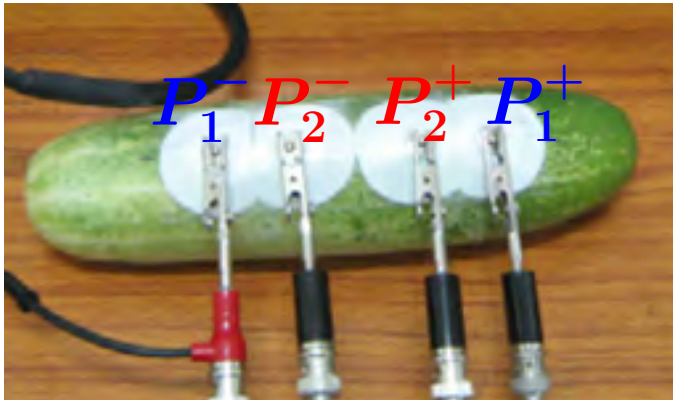

Let u^j $(j = 1, 2)$ satisfy

$$\begin{cases} \nabla \cdot (\gamma \nabla u^j) = 0 \text{ in } \Omega \\ \gamma \frac{\partial u^j}{\partial \nu} | \partial\Omega = g_j \end{cases}$$

† $g_j := I(\delta(P_j^+ - \cdot) - \delta(P_j^- - \cdot))$

$$\gamma = \underbrace{\left[u^1(P_2^+) - u^1(P_2^-)\right]/I}_{Z^{1,2} \text{ (measurable quantity)}} \underbrace{\left(\int_\Omega \nabla u^1 \cdot \nabla u^2 dx\right)^{-1}}_{\text{to be computed}}$$

- How to compute $\int_\Omega \nabla u^1 \cdot \nabla u^2 dx$?
- **Impedance $Z^{1,2}$** depends mainly on **electrode positions ($P_1^\pm, P_2^\pm$) & the geometry of Ω. Why? How?**
- γ changes with ω. **Why? How?**

Use Neumann function N_Ω to measure γ

The relation between impedance Z & impedivity γ^{-1} is influenced by the geometry $\partial\Omega$ & electrode positions $P_j^{\pm}$.

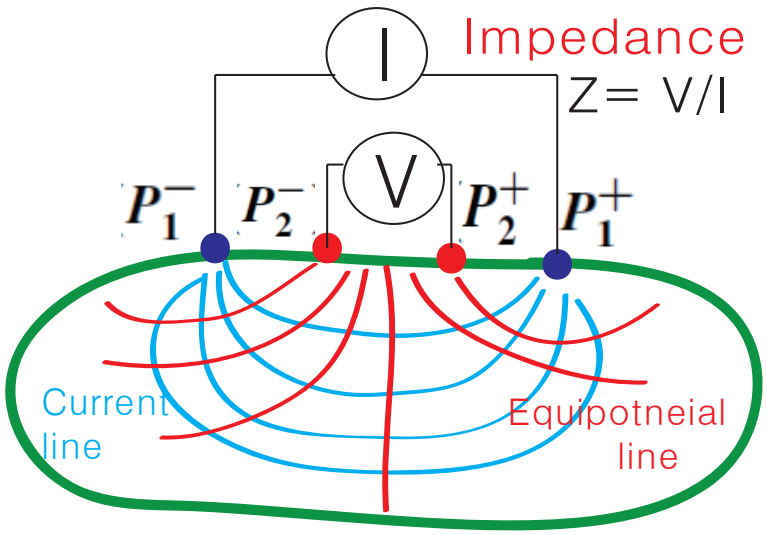

$$\gamma = \frac{1}{u^1(P_2^{\pm})} \underbrace{\int_{\partial\Omega} N_\Omega(P_2^{\pm}, y) g_1(y) ds_y}_{\gamma\, u^1(P_2^{\pm})}$$

$$\begin{cases} \nabla \cdot (\gamma \nabla u^1) = 0 \ \text{ in } \Omega \\ \gamma \frac{\partial u^1}{\partial \nu}|_{\partial\Omega} = \delta(P_1^+ - \cdot) - \delta(P_1^- - \cdot) \end{cases}$$

Neumann function N_Ω depends sensitively on the geometry $\partial\Omega$:

$$\mathcal{S}(-\frac{1}{2}I + \mathcal{K}^*)^{-1} = I \ \rightsquigarrow \ N_\Omega = (-\frac{1}{2}I + \mathcal{K})^{-1}\Phi$$

$\ast \Phi(x,y) := \frac{1}{4\pi|x-y|}, \quad \mathcal{S}f(x) := \int_{\partial\Omega} \Phi(x,y) f(y) ds_y,$

$\ast\ \mathcal{K} : L^2(\partial\Omega) \to L^2(\partial\Omega)$ defined by $\mathcal{K}f(x) := \int_{\partial\Omega} \frac{\partial}{\partial \nu_y} \Phi(x,y) f(y) ds_y$

Both $\sigma = \Re\{\gamma\}$ and $\epsilon = \Im\{\gamma/\omega\}$ in $\nabla(\gamma\nabla u) = 0$ change with ω because of non-conducting cell membrane.

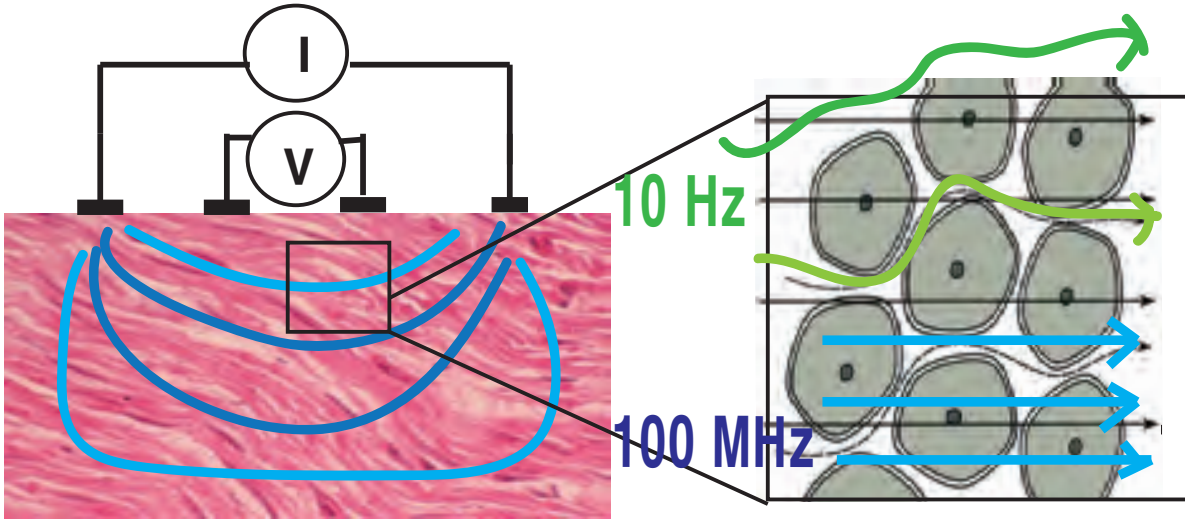

$$\gamma = cI/V$$
$$\sigma = c\Re\{I/V\}$$
$$\epsilon = c\frac{1}{\omega}\Im\{I/V\}$$

- c depends on the geometry $\partial\Omega$ and electrode positions.
- **Low frequency currents are blocked by the nonconducting membrane so it pass through extras cellular fluid. High frequency currents pass through the membranes. Why?**
  - ✓ $\left|\frac{\gamma|_{membrane}}{\gamma|_{background}}\right| \approx 0$ at 10 Hz, whereas $\left|\frac{\gamma|_{membrane}}{\gamma|_{background}}\right| \gtrapprox 0$ at 100MHz.

ω-dependent effective γ can be estimated by the use of double layer (membrane) potential via homogenization.

ω-dependent effective γ is expressed as

$$\gamma_{(\text{effective})} = [\gamma_{ij}] = \gamma_0 \left[\delta_{ij} - \frac{\gamma_0 d}{\gamma_m} \int_\Gamma \nu_j (I + \frac{\gamma_0 d}{\gamma_m} \mathcal{T})^{-1} \nu_i ds \right]$$

$$\mathcal{T}[\phi] = \frac{\partial}{\partial \nu} \int_\Gamma \frac{\partial}{\partial \nu_y} \underbrace{G(\cdot - y)}_{Green} \phi(y) ds_y$$

[Ammari, Garnier, Giovangigli, Jing, Seo, Spectroscopic imaging of a dilute cell suspension, JEMS 2015]

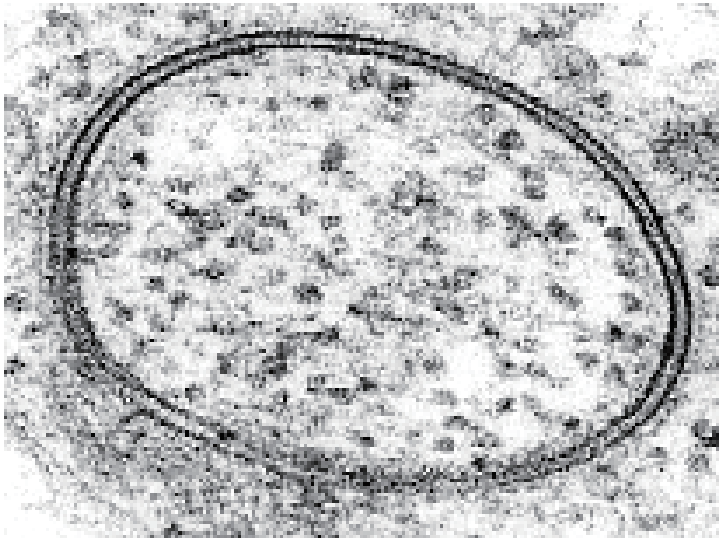

- $\frac{\gamma_0 d}{\gamma_m} = \frac{\sigma_0 d}{\sigma_m} \gg 0$ at $\omega = 0$
  $\rightsquigarrow$ **anisotropic γ**
- $\frac{\gamma_0 d}{\gamma_m} = \frac{d(\sigma_0 + i\omega\epsilon_0)}{\sigma_m + i\omega\epsilon_m} \approx 0$ at $\omega = 10^8$
  $\rightsquigarrow$ **isotropic γ**
- Γ:=membrane surface
- d :=thickness of membrane
- $\gamma_m := \gamma|_{membrane}$, $\gamma_0 := \gamma|_{background}$

Human Experiments with Multiple Electrodes

Admittivity $\gamma := \sigma + i\omega\epsilon$ **& potential** u are connected by

$$\nabla \cdot (\gamma \nabla u) = 0 \quad \text{in a human body } \Omega$$

- **Effective impedivity** γ^{-1} (3×3 matrix) depends on scale and ω.
- **Impedance** $Z^{j,k}$ (**measurable quantity**; see the figure below) is the ratio between j−th current (injected by j-th pair of electrodes) and the induced potential difference between the k-th pair:

$$Z^{j,k} = \frac{V^{j,k}}{I} = \frac{1}{I^2} \int_\Omega \gamma \nabla u^j \cdot \nabla u^k dx$$

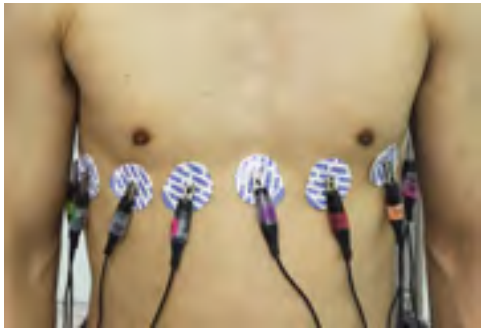

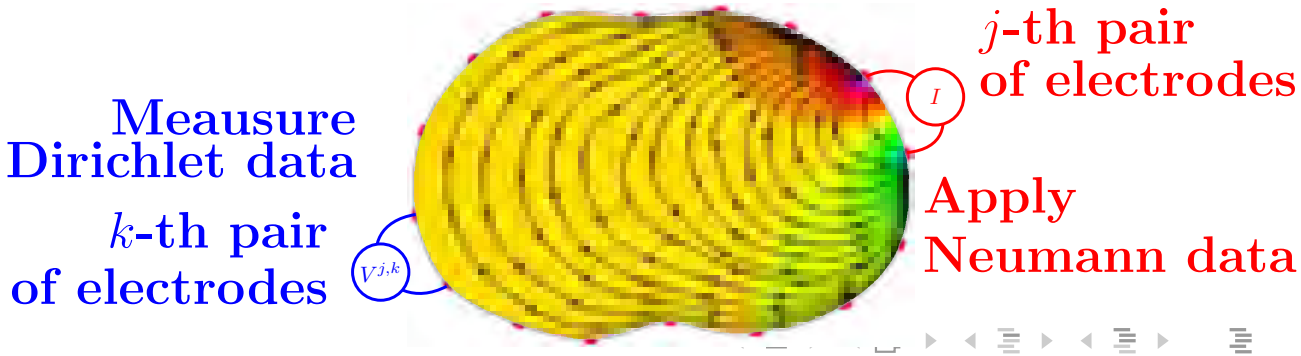

Body Impedance Measurement (Not Tomography)

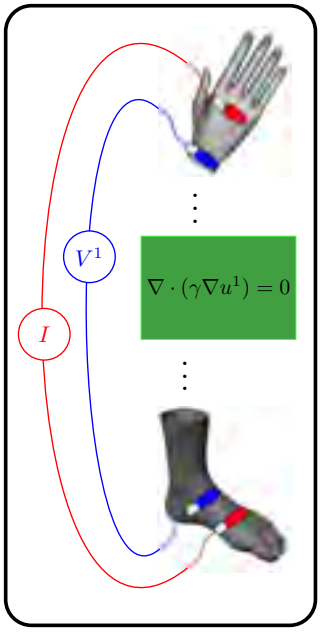

(a)

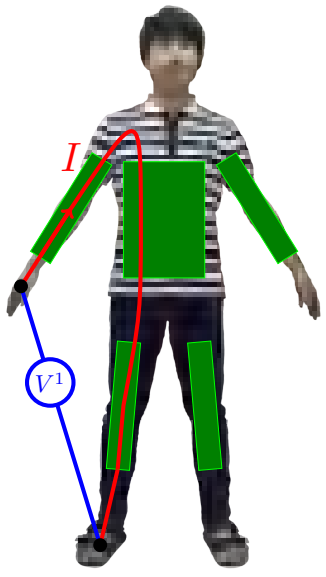

$$Z^1_{\text{body}} \approx \frac{(Z^1+Z^2)-(Z^3+Z^4)}{2}$$

$$Z^j = \frac{V^j}{I} = \frac{1}{I^2}\int_\Omega \frac{1}{\gamma}\left|\gamma \nabla u^j\right|^2 d\mathbf{x} : \text{measurable}$$

$$Z^1 \approx \frac{1}{I^2}\int_{\Omega_{\text{ra}}} \frac{1}{\gamma}\left|\gamma \nabla u^1\right|^2 d\mathbf{x} + \frac{1}{I^2}\int_{\Omega_{\text{body}}} \frac{1}{\gamma}\left|\gamma \nabla u^1\right|^2 d\mathbf{x} + \frac{1}{I^2}\int_{\Omega_{\text{rl}}} \frac{1}{\gamma}\left|\gamma \nabla u^1\right|^2 d\mathbf{x}$$

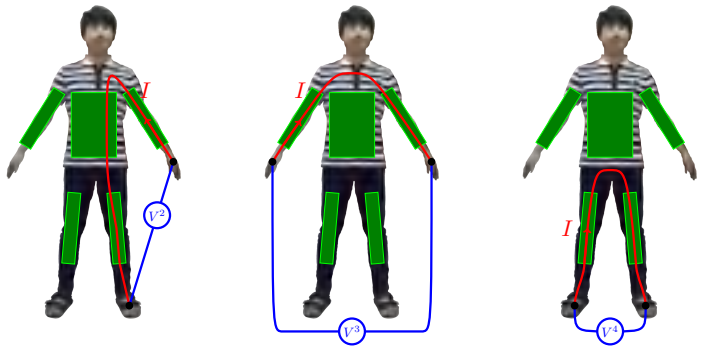

(b)

Human body Ω can be decomposed into five parts. **The commercial system (InBody) calculates the volume of the body water by**

$$\frac{1}{I^2}\int_{\Omega_{body}} \gamma|\nabla u^1|^2 dx = \underbrace{\frac{1}{2}(Z^1 + Z^2 - Z^3 - Z^4)}$$

Eliminate contributions of legs and arms

This method reduces electrode position uncertainties! Why?

Electrical Impedance Tomography - 16 channel EIT

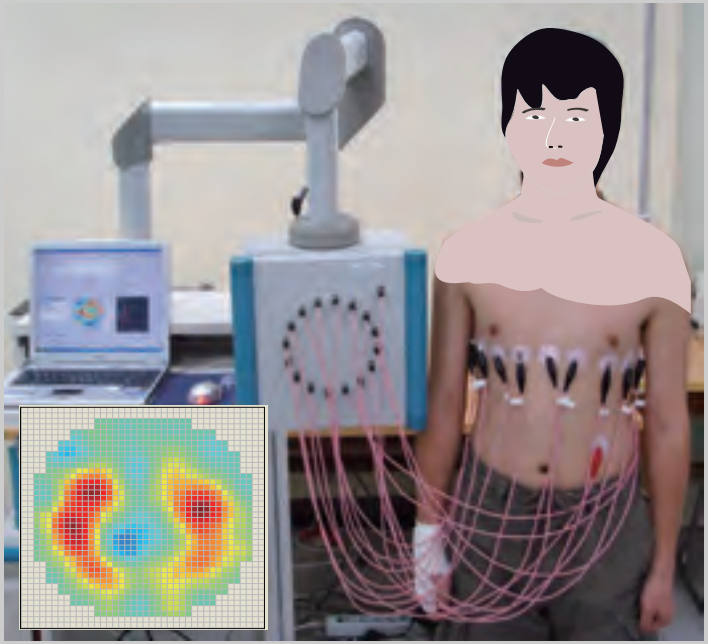

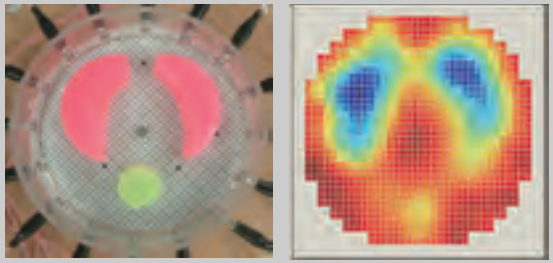

Time-difference EIT

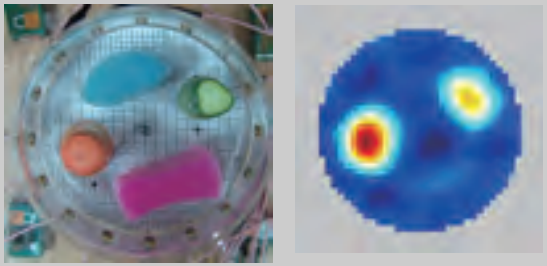

Frequency difference EIT

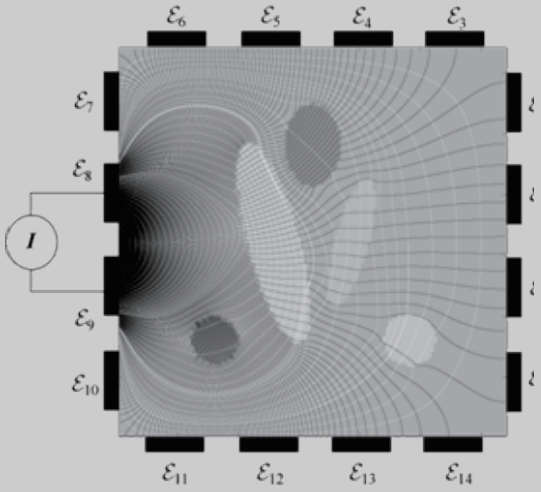

16 channel EIT

u^j :=potential due to j-th injection current:

$$\begin{cases} \nabla \cdot (\gamma \nabla u^j) = 0 & \text{in } \Omega \\ (u + z_k \gamma \frac{\partial u}{\partial \mathbf{n}})|\mathcal{E}_k = U_k, \quad k = 1, \cdots, E \\ \gamma \frac{\partial u^j}{\partial \mathbf{n}} = 0 & \text{on } \partial\Omega \setminus \cup_{k=1}^{16} \mathcal{E}_k \\ \int_{\mathcal{E}_k} \gamma \frac{\partial u}{\partial \mathbf{n}} = 0 & \text{if } k \neq j, j+1 \\ \int_{\mathcal{E}_j} \gamma \frac{\partial u^j}{\partial \mathbf{n}} \, ds = I = -\int_{\mathcal{E}_{j+1}} \gamma \frac{\partial u^j}{\partial \mathbf{n}} \, ds \end{cases}$$

where z_k is the contact impedance of the kth electrode $\mathcal{E}_k$ and U_k is the voltage on $\mathcal{E}_k$.

Measured EIT data is

$$\mathbb{F} = \left[V^{1,1}, \cdots, V^{1,16}, \cdots\cdots, V^{j,k}, \cdots, \cdots \right]^T$$

where

$$V^{j,k} := U_k^j - U_{k+1}^j$$

History of EIT

- Henderson and Webster (1978): EIT by designing the impedance camera.
- Calderón (1980): Mathematical inverse problem to identify σ entering $\nabla \cdot (\sigma \nabla u) = 0$ in a domain Ω from the knowledge of NtD map.
- Barber and Brown (1982) developed an EIT version of the CT back-projection algorithm. The first EIT device (Sheffield Mark 1) with one active current source.
- Isaacson (1986) suggested the concept of distinguishability. RPI group developed EIT system with multiple active current sources to maximize the distinguishability.
- Dräger and Swisstom (2010-) developed commercial EIT systems for visualizing the regional distribution of ventilation in the lungs continuously, without radiation, and directly at the patients bedside.

Electrical Impedance Tomography

Reconstruct $\gamma = \sigma + i\omega\epsilon$ at each ω and time t. If it is too difficult, reconstruct its changes:

$$\frac{\partial}{\partial t}\gamma \quad \& \quad \frac{\partial}{\partial \omega}\gamma$$

⁎ Note that σ and ϵ depend on position $\mathbf{x}$, ω, and t.

Measured Data: $Z^{j,k} = \frac{V^{j,k}}{I} = \frac{1}{I^2}\int_\Omega \gamma \nabla u^j \cdot \nabla u^k d\mathbf{x}, \ (\forall |j-k| > 1)$

$\frac{\partial}{\partial t}\gamma$ **Time-difference EIT**

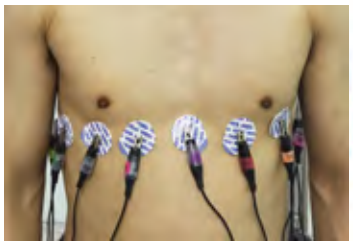

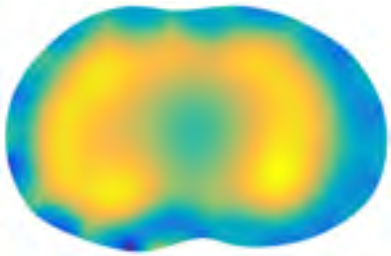

$\frac{\partial}{\partial \omega}\gamma$ **Frequency-difference EIT**

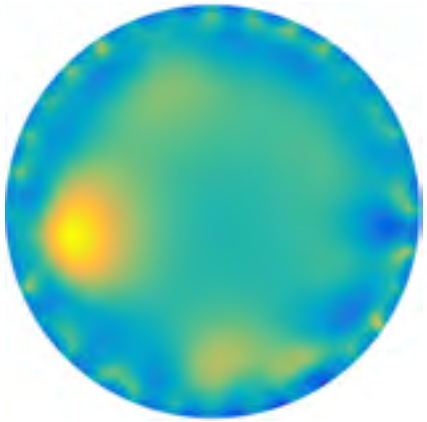

Reciprocity Principle: $Z^{j,k} = Z^{k,j}$.

$$\underbrace{u^8(P_3,\omega,t) - u^8(P_2,\omega,t)}_{Z^{8,2}\leftarrow\text{measured data}} = \int_\Omega \gamma \nabla u^8 \cdot \nabla u^2 dr = \underbrace{u^2(P_9,\omega,t) - u^2(P_8,\omega,t)}_{Z^{2,8}\leftarrow\text{measured data}}$$

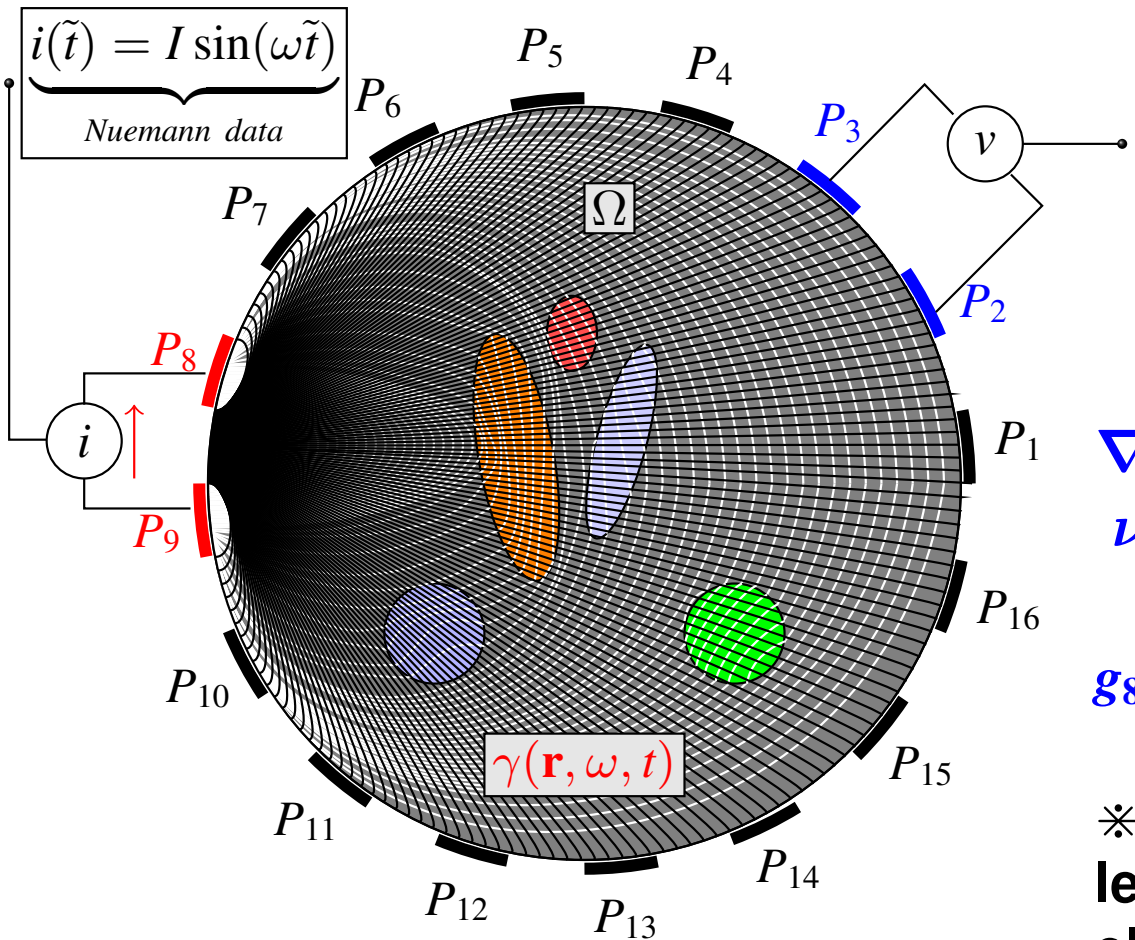

stream and equipotential lines for 16 ch.phantom

$$\underbrace{u^8(P_3,\omega,t) - u^8(P_2,\omega,t)}_{\text{Dirichlet data}}$$

$$\nabla\cdot(\gamma\nabla u^8) = 0 \text{ in } \Omega$$
$$\nu\cdot(\gamma\nabla u^8)|_{\partial\Omega} = g_8$$

$$g_8 = \delta(\cdot - P_9) - \delta(\cdot - P_8)$$

※ **For the ease of explanation, let $I = 1$mA and use the point electrode model.**

EIT Reconstruction Algorithm

tdEIT aims to reconstruct $\frac{\partial}{\partial t}\gamma$ from $\frac{d}{dt}Z^{j,k}$ & the relation

$$\underbrace{\frac{d}{dt}Z^{j,k}}_{\frac{d}{dt}V^{j,k}} \approx \int_\Omega \frac{\partial \gamma}{\partial t}\nabla u^j \cdot \nabla u^k dx \approx \underbrace{\sum_m \int_{\Omega_m} \frac{\partial \gamma}{\partial t}\nabla u^j \cdot \nabla u^k dx}_{\text{N(j-1)+k-component of } \mathbf{S}\frac{\partial \gamma}{\partial t}}$$

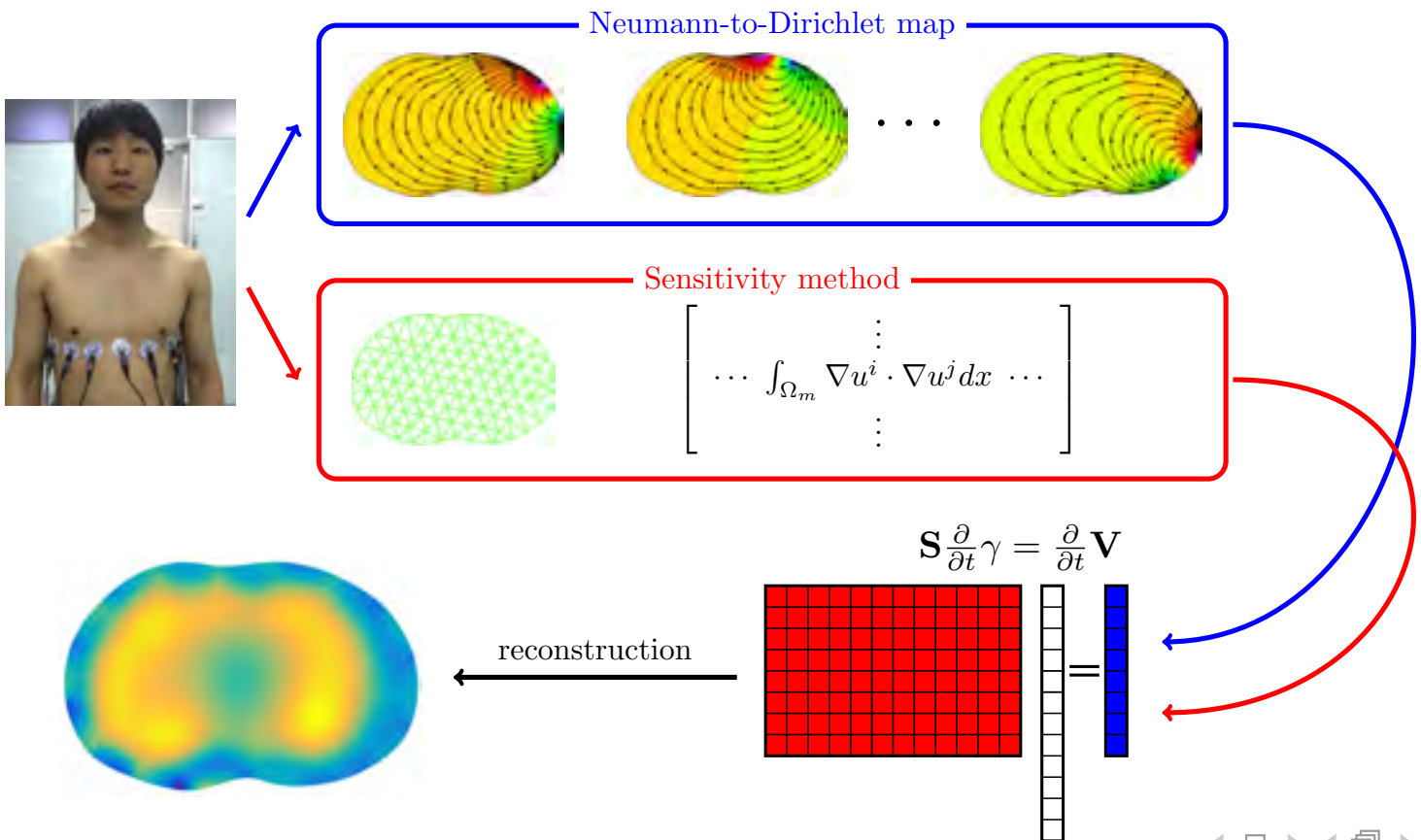

Sensitivity matrix depends on electrode displacement, arrangement of injection current, mesh structure, and the boundary geometry. Data $Z^{j,j-1}$, $Z^{j,j}$, $Z^{j,j+1}$ are not reliable due to electrode contact impedance uncertainty.

EIT: Linearized Method

$$\underbrace{\frac{d}{dt}V^{j,k}}_{data} \approx \int_\Omega \frac{\partial}{\partial t}\gamma \nabla u^j \cdot \nabla u^k dx \approx \sum_m \underbrace{\int_{\Omega_m} \nabla u_0^j \cdot \nabla u_0^k dx}_{s_{N(j-1)+k,m}} \frac{\partial}{\partial t}\gamma|_{\Omega_m}$$

Find a suitable linear combination of column vectors $(s_{N(j-1)+k,1}), \cdots, (s_{N(j-1)+k,1})$ which matches with the data $\frac{d}{dt}(V^{1,1}, \cdots, V^{N,N})$.

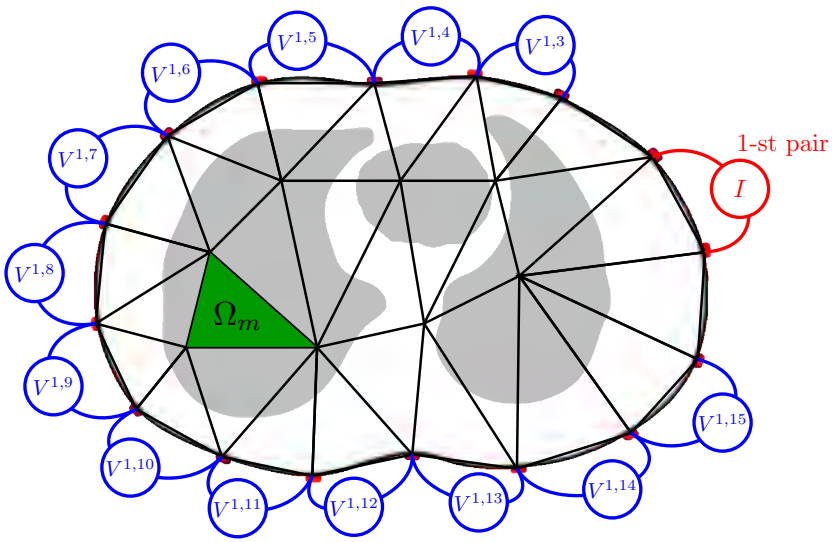

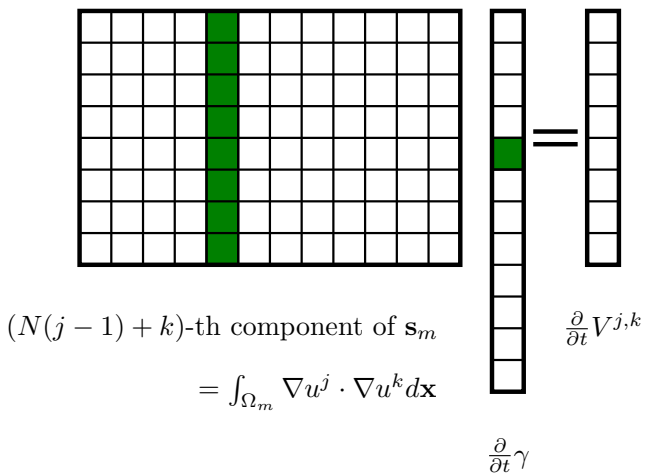

⁕ **Inclusion detection of recovering $\cup\{\Omega_m : \frac{d}{dt}\gamma_m \neq 0\}$ is linear.....**

[Harrach/S, SIAMA 2010]

Positive, Zero, Negative Sensitivity

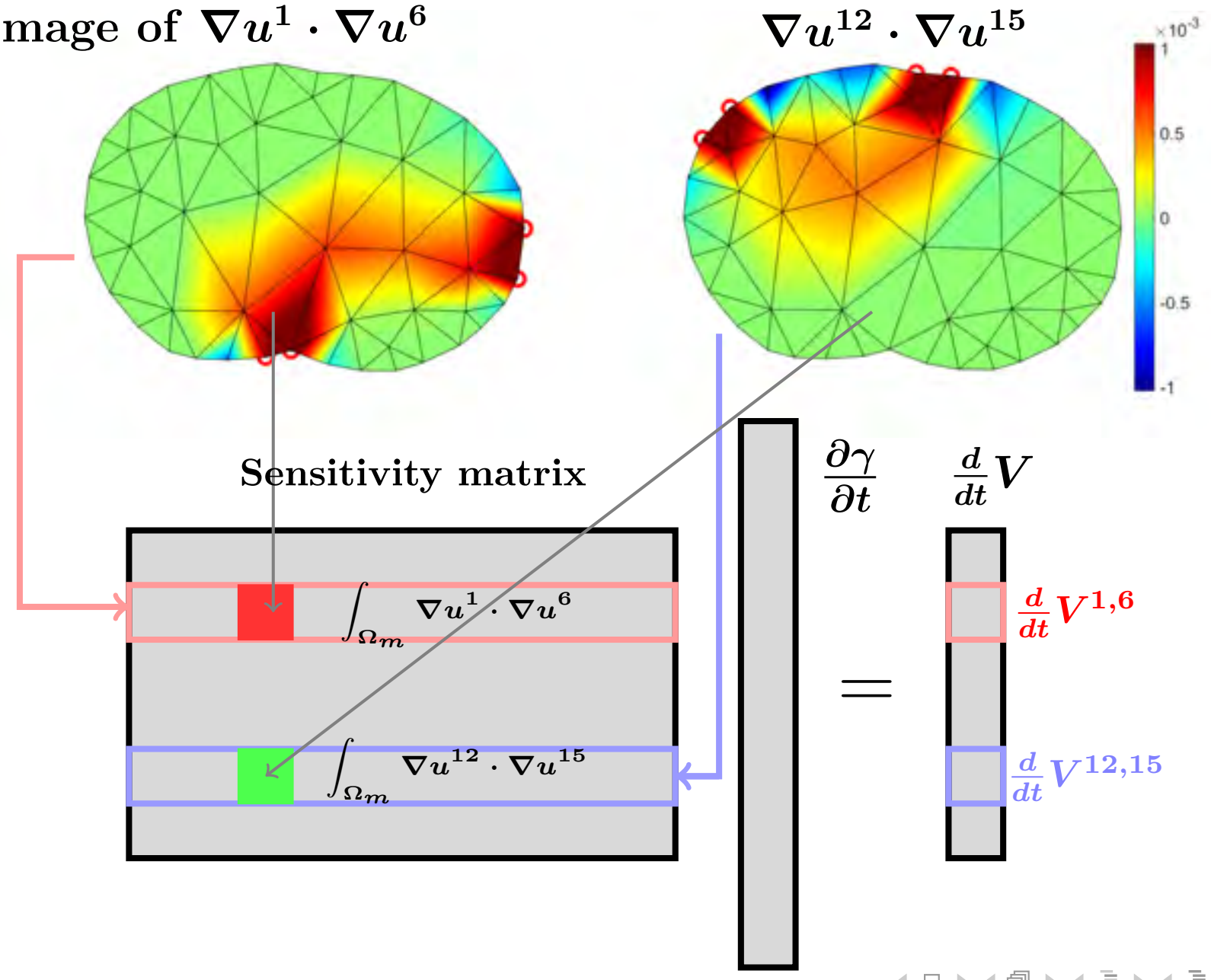

Static EIT is severely ill-posed.

EIT data $\mathbf{V}$ depends mainly on the boundary geometry and the electrode positions, whereas its dependence on a local perturbation of γ is relatively small. See the structure of eigenvectors of EIT Sensitivity matrix.

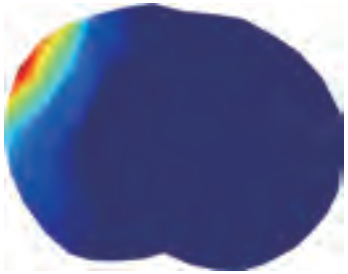

λ_1

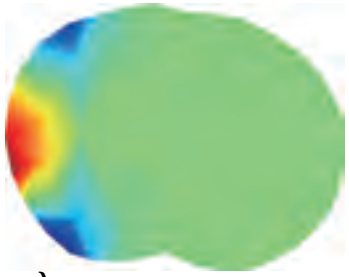

$\frac{\lambda_5}{\lambda_1} = 0.8599$

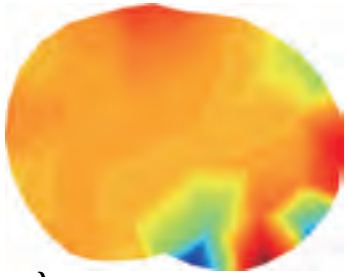

$\frac{\lambda_{10}}{\lambda_1} = 0.6626$

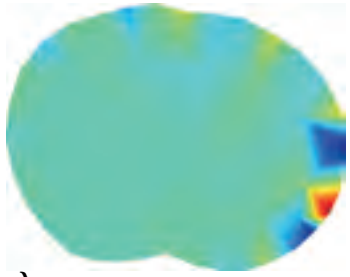

$\frac{\lambda_{20}}{\lambda_1} = 0.4384$

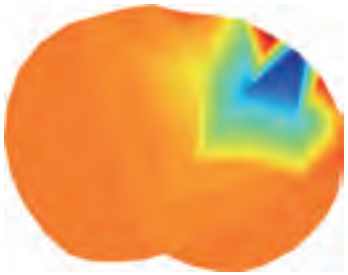

$\frac{\lambda_{40}}{\lambda_1} = 0.0328$

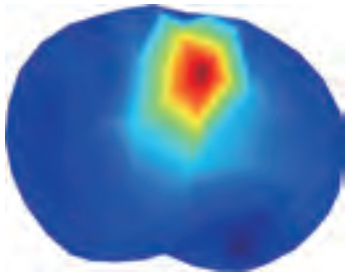

$\frac{\lambda_{50}}{\lambda_1} = 0.0049$

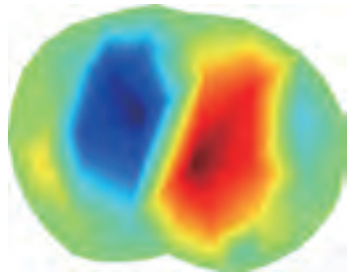

$\frac{\lambda_{60}}{\lambda_1} = 0.0009$

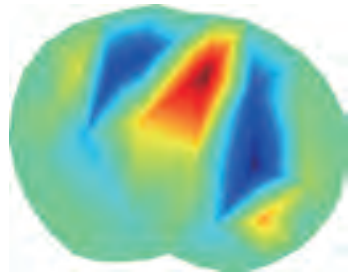

$\frac{\lambda_{70}}{\lambda_1} = 0.0001$

Lung EIT to monitor $\frac{\partial \gamma}{\partial t}$ from $\frac{d}{dt} V^{j,k}$

EIT has its unique ability to allow long-term, continuous monitoring of lung ventilation at the bedside. Lung EIT aims to provide dynamic images of $\frac{\partial \gamma}{\partial t}$ from

$$\frac{d}{dt} V^{j,k} \approx \int_{\Omega} \frac{\partial \gamma}{\partial t} \nabla u^j \cdot \nabla u^k d\mathbf{x}, \qquad \forall |j-k| > 1$$

.

Swisstom: BB2

Get Ω & electrode positions.

It is important to match Ω to the patient's geometry, in order to use the relation $V^{j,k} = \int_\Omega \gamma \nabla w^j \cdot \nabla u^k dx$ effectively.

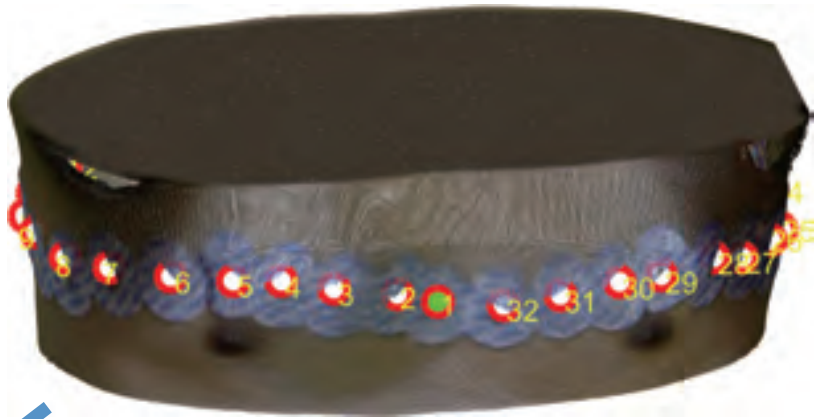

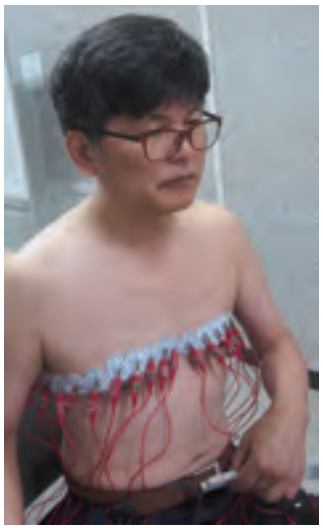

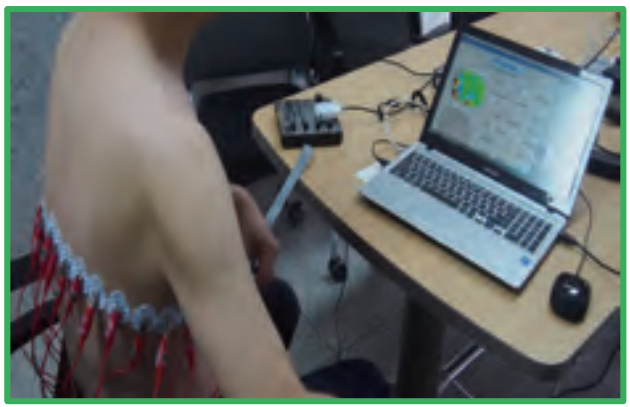

Reduce the forward modeling errors.

Thanks to rapid development of 3D scanning, we have a chance to alleviate the forward modelling error including electrode position P_j and boundary geometry $\partial\Omega$. We cannot deal with the uncertainty of the reference conductivity distribution γ_0.

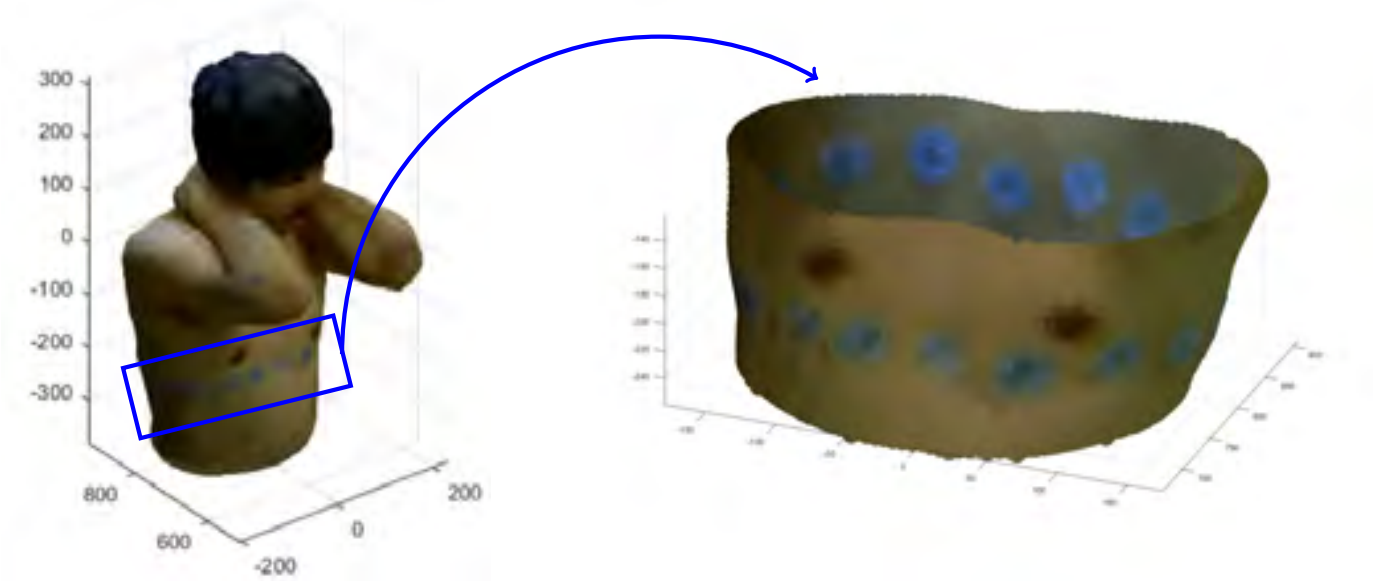

Barber and Brown's observation: If electrodes are spaced 10 cm apart around the thorax, variation in positioning of 1 mm will produce errors of 1% in the data V.

Combine spatial and temporal regularization to deal with the ill-posed nature.

Enforcing the temporal monotonic constraint on lung ventilation-related conductivity change, the corresponding inverse problem becomes better posed.

- Decompose $\frac{\partial}{\partial t}\sigma$ into ventilation and parts

$$\frac{\partial}{\partial t}\sigma^t(x) = \underbrace{\frac{\partial}{\partial t}\sigma_L}_{\text{ventilation}} + \underbrace{\frac{\partial}{\partial t}\sigma_H}_{\text{others}} \quad x \in \Omega.$$

- Use a band-pass filter to extract the ventilation-related signal :

$$\frac{d}{dt}V_L^{j,k}(t) \approx -\int_\Omega \frac{\partial \sigma_L^t}{\partial t}\nabla u^j \cdot \nabla u^k dx$$

[Liangdong Zhou & Bastian Harrach, Seo; Monotonicity-based Electrical Impedance Tomography Lung Imaging(2015)]

Monotonic assumption on the ventilation-related conductivity variation

Under this assumption, the ventilation-related data $\mathbb{V}_L$ (N-channel EIT system) is **either positive or negative semidefinite** matrix:

$$\mathbb{V}_L(t) = \begin{bmatrix} V_L^{1,1}(t) & \cdots & V_L^{1,N}(t) \\ V_L^{2,1}(t) & \cdots & V_L^{2,N}(t) \\ \vdots & \ddots & \vdots \\ V_L^{N,1}(t) & \cdots & V_L^{N,N}(t) \end{bmatrix}.$$

To determine whether the matrix $\frac{d}{dt}\mathbb{V}_L(t)$ is positive or negative semi-definite, we use the formula:

$$\mathbf{a}^T \frac{d}{dt}\mathbb{V}_L(t)\mathbf{a} = -\int_\Omega \frac{\partial \sigma_L}{\partial t} \nabla\Big(\sum_j a_j u^j\Big) \cdot \nabla\Big(\sum_k a_k u^k\Big) dx$$

for all $\mathbf{a} = (a_1, \cdots, a_N)^T \in \mathbb{R}^N$.

Remarkable EIT data pattern in human experiments

- $\inf_{x\in\Omega} \frac{\partial \sigma_L}{\partial t}(x) \geq 0 \;\Rightarrow\; \frac{d}{dt}\mathbb{V}_L \precapprox \mathbf{0}$ (positive-semidefinite)
- $\sup_{x\in\Omega} \frac{\partial \sigma_L}{\partial t}(x) \leq 0 \;\Rightarrow\; \frac{d}{dt}\mathbb{V}_L \succapprox \mathbf{0}$ (negative-semidefinite)

Observation: $\widetilde{V}^{j,k}(t)$ have a similar time-varying pattern:

$$\widetilde{V}^{j,k}(t) := \frac{V^{j,k}(t)}{\text{sign}\left(\int_\Omega \nabla w^j \cdot \nabla u^k\right)} + \left(1 - \text{sign}\left(\int_\Omega \nabla w^j \cdot \nabla u^k\right)\right)\text{ave}V^{j,k}$$

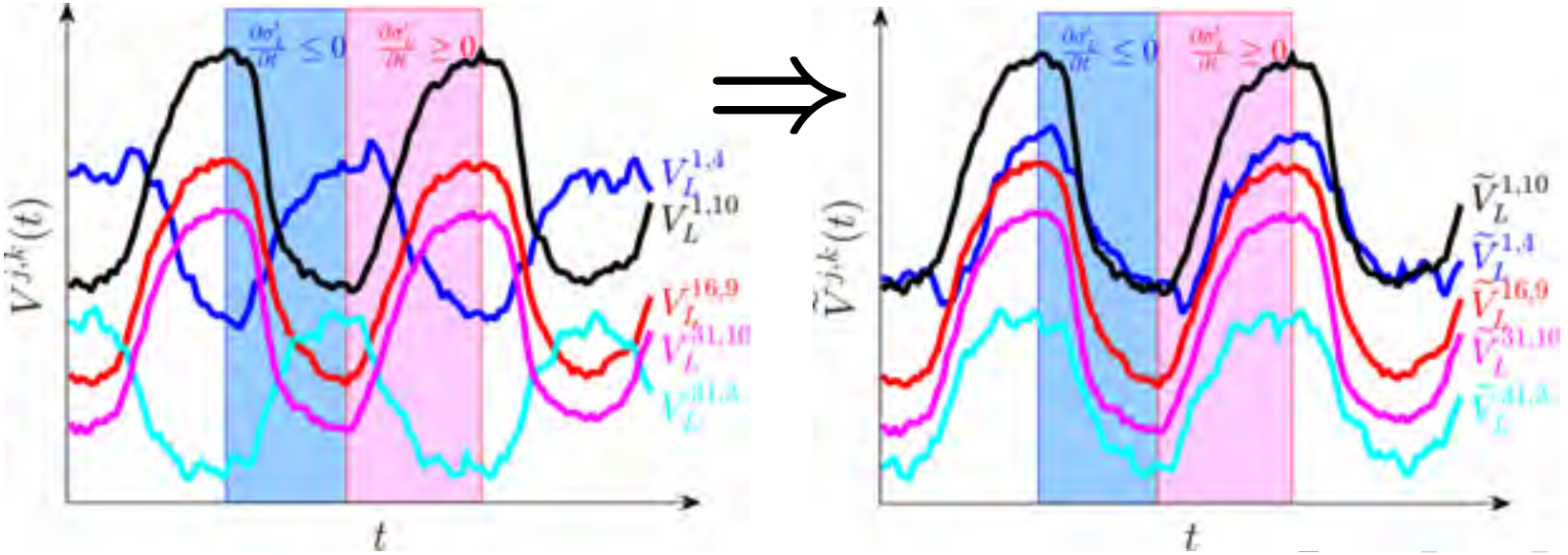

MREIT for recovering σ

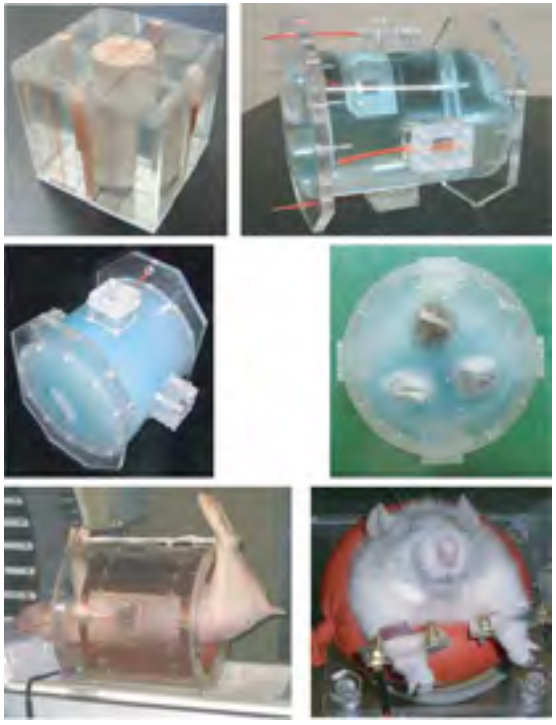

Imaging Objects

MRI Scanner

Current Source

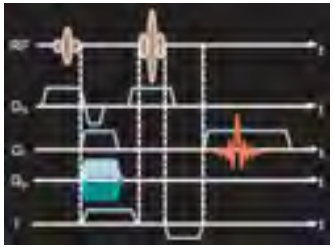

Pulse Sequence

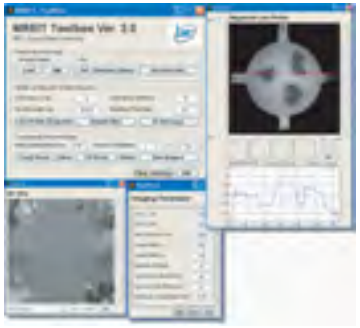

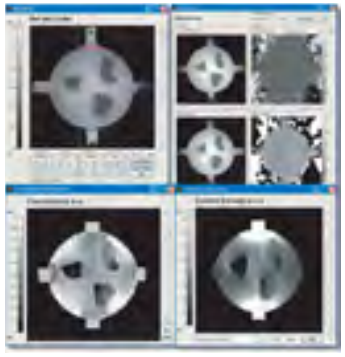

Image Reconstruction Software

MREIT aims to provide σ using MRI. EIT data is insufficient to provide σ.

MREIT Math. Model

When modeling, we must take account of **well-posedness (Uniqueness, Existence, Stability)**.

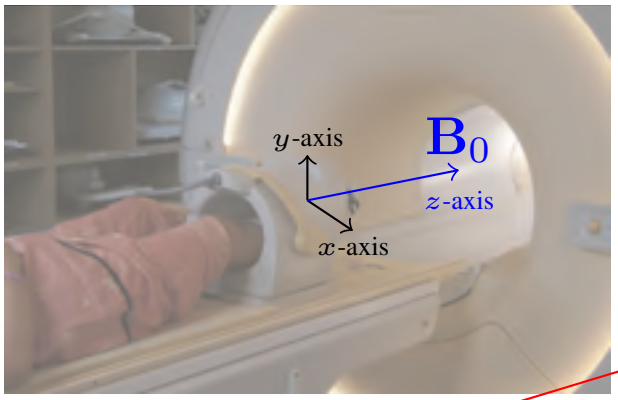

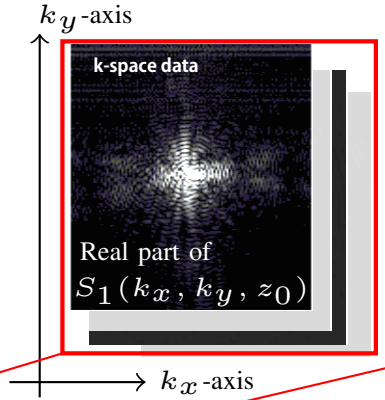

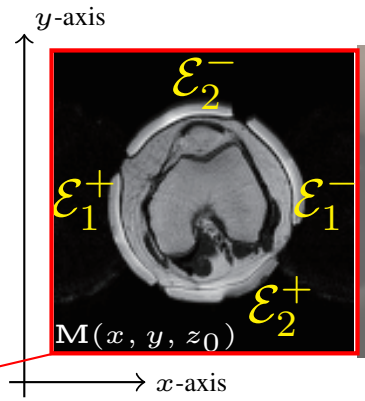

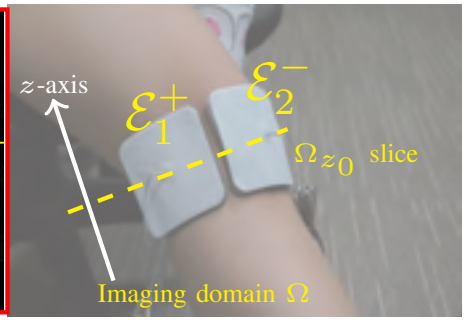

$$S_j(k_x, k_y, z_0) = \int_{\Omega_{z_0}} M(x, y, z_0) e^{i\delta(x,y,z_0)} e^{i\gamma T_c B_{z,j}(x,y,z_0)} e^{i(xk_x + yk_y)} dS_{xy}$$

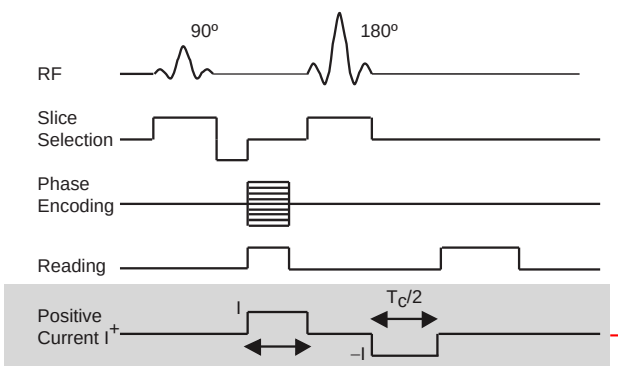

$$\frac{1}{\mu_0} \nabla \times \mathbf{B}_j = -\sigma \nabla u_j$$

$$I = \pm \int_{\mathcal{E}_j^{\pm}} \sigma \nabla u_j \cdot \mathbf{n} \, ds$$

$$(j = 1, 2)$$

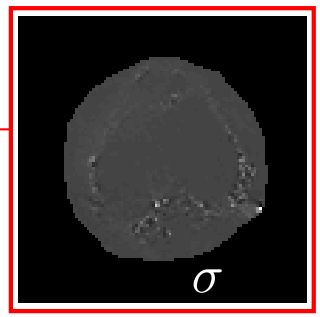

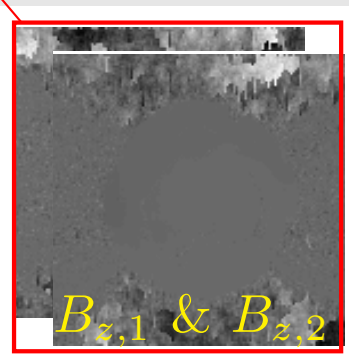

MREIT aims to visualize σ.

- Both EIT and MREIT use a pair of electrodes $\mathcal{E}^+$ and $\mathcal{E}^-$ to produces $\mathbf{J} = (J_x, J_y, J_z)$ and $\mathbf{B} = (B_x, B_y, B_z)$. The relation among $\sigma, \mathbf{J}, \mathbf{B}$ is

$$-\sigma \nabla u = \mathbf{J} = \frac{1}{\mu_0} \nabla \times \mathbf{B}$$

- **EIT vs MREIT**:
  - EIT uses electrodes to get boundary measurements.
  - MREIT uses MRI to get the internal data B_z, z-component of $\mathbf{B} = (B_x, B_y, B_z)$.

How to measure B_z. (1989, Joy *et al*, Toronto Group)

MRI scanner can provide the complex k-space MR signal $S(k_x, k_y)$ involving B_z on the slice $\Omega_{z_0} = \Omega \cap \{z = z_0\}$:

$$S(k_x, k_y) = \int\int_{\Omega_{z_0}} M(x, y, z_0) e^{i(\eta B_z(x,y,z_0) T_c + \delta(x,y,z_0))} e^{i(xk_x + yk_y)} dxdy$$

Fourier transform of $S(k_x, k_y)$ $\rightsquigarrow$

$$\mathcal{M}(x, y, z_0) := M(x, y, z_0)\ e^{i\eta B_z(x,y,z_0) T_c}\ e^{i\delta(x,y,z_0)}.$$

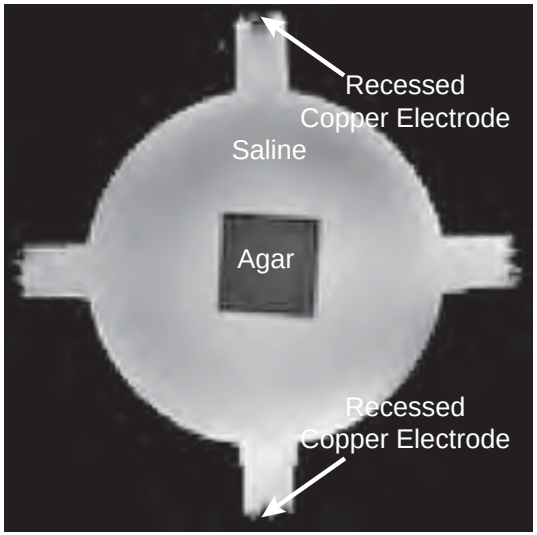

(a)$M(x, y, z_0)$

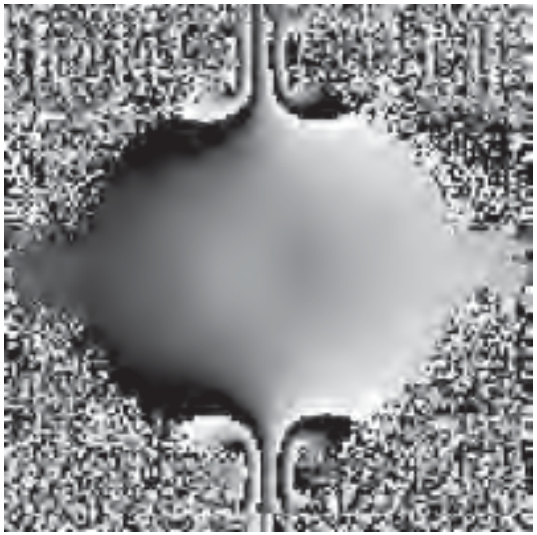

(b)wrapped B_z

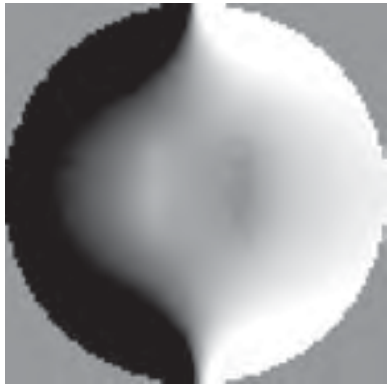

(c) B_z

MREIT using full components of $\mathbf{H}$:

Major drawback: It requires subject rotation inside MRI scanner.

- Least square method
  [Zhang 1992]

$$\min_{\sigma} \frac{1}{2} \| \nabla \times \mathbf{H} + \sigma \nabla u \|^2$$

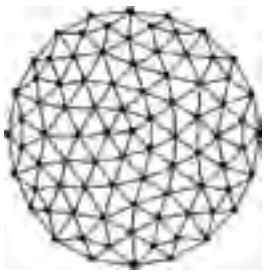

Finite element model

True $1/\sigma$

Reconstructed $1/\sigma$

Low spatial resolution

[Woo, Lee, Moon 1994], [Idel and Birgul 1995]

- $J-$substitution method
  [Kwon, Seo, Yoon, Woo 2001]

$$\nabla \cdot \left(\frac{|\mathbf{J}|}{|\nabla u|} \nabla u \right) = 0$$

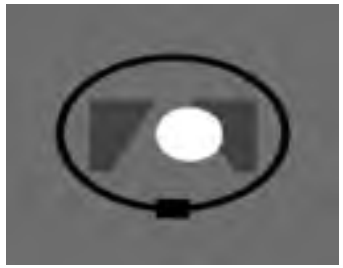

True $1/\sigma$

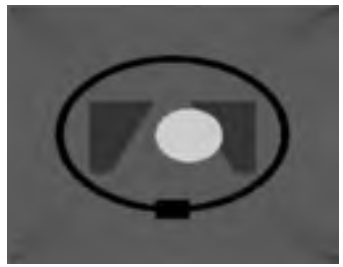

Reconstructed $1/\sigma$

High spatial resolution

In 2005-present, CDII by Nachman, Tamasan, Timonov, Joy

Inverse Problem of MREIT

Recover σ from the B_z data as a function of σ and Neumann data g:

$$\Lambda_\sigma(g)(\mathbf{r}) := \frac{\mu_0}{4\pi}\int_\Omega \frac{\sigma(\mathbf{r}')\,[(x-x')\frac{\partial u}{\partial y}(\mathbf{r}') - (y-y')\frac{\partial u}{\partial x}(\mathbf{r}')]}{|\mathbf{r}-\mathbf{r}'|^3}\,d\mathbf{r}'$$

where u satisfies

$$\begin{cases} \nabla\cdot(\sigma\nabla u) = 0 \quad \text{in} \quad \Omega \\ \sigma\frac{\partial u}{\partial \nu}|_{\partial\Omega} = g \end{cases}$$

Conductivity

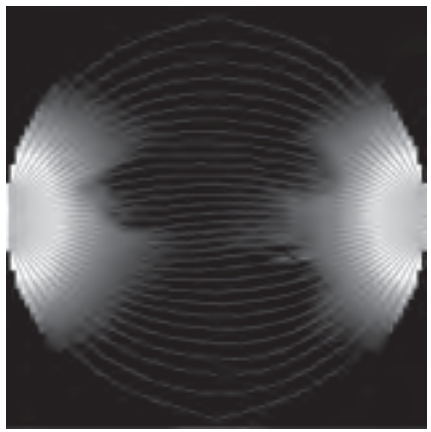

Current Density

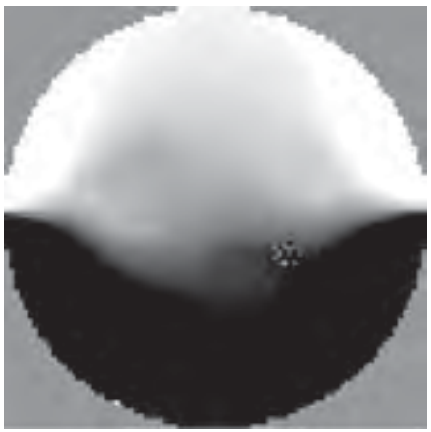

Bz-data

Relation between σ and $\Lambda_\sigma(g) = B_z$

- From Ampere's law $\mathbf{J} = \frac{1}{\mu_0}\nabla \times \mathbf{B}$,

$$\mu_0 \nabla \times \mathbf{J} = \nabla \times \nabla \times \mathbf{B} = -\nabla^2 \mathbf{B} + \nabla \underbrace{\nabla \cdot \mathbf{B}}_{=0} = -\nabla^2 \mathbf{B}$$

- $\nabla \times \mathbf{J} = -\nabla \times [\sigma \nabla u] = -\nabla \sigma \times \nabla u - \underbrace{\sigma \nabla \times \nabla u}_{=0}$
- Denoting $\hat{\mathbf{z}} = (0, 0, 1)$,

$$\frac{1}{\mu_0}\nabla^2 B_z = \hat{\mathbf{z}} \cdot \nabla \sigma \times \nabla u = \mathbf{d} \cdot \nabla \sigma \qquad (\mathbf{d}(\mathbf{r}) := \hat{\mathbf{z}} \times \nabla u(\mathbf{r}))$$

  - **If B_z is convex at $\mathbf{r}$, then $\sigma(\mathbf{r}) \nearrow$ in $\mathbf{d}(\mathbf{r})$-direction.**
  - **If B_z is concave at $\mathbf{r}$, then $\sigma(\mathbf{r}) \searrow$ in $\mathbf{d}(\mathbf{r})$-direction.**
  - **If $\nabla^2 B_z(\mathbf{r}) = 0$, then $\sigma(\mathbf{r})$ does not change in $\mathbf{d}(\mathbf{r})$-direction.**

Key observation

✓ B_z **is blind to** $\nabla_{xy} u \cdot \nabla_{xy} \sigma$**.**

Non-uniqueness theorem

For a given $g \in H^{-1/2}(\partial\Omega)$ and a conductivity σ, $\exists$ infinitely many $\tilde{\sigma}$ such that

$$\Lambda_{\tilde{\sigma}}[g] = \Lambda_{\sigma}[g] \quad \text{in } \Omega$$

σ (left) and $\tilde{\sigma}$ (right) produce the same B_z.
Here, $\tilde{\sigma} := \frac{\sigma}{\phi'(u)}$ with ϕ being an increasing function.

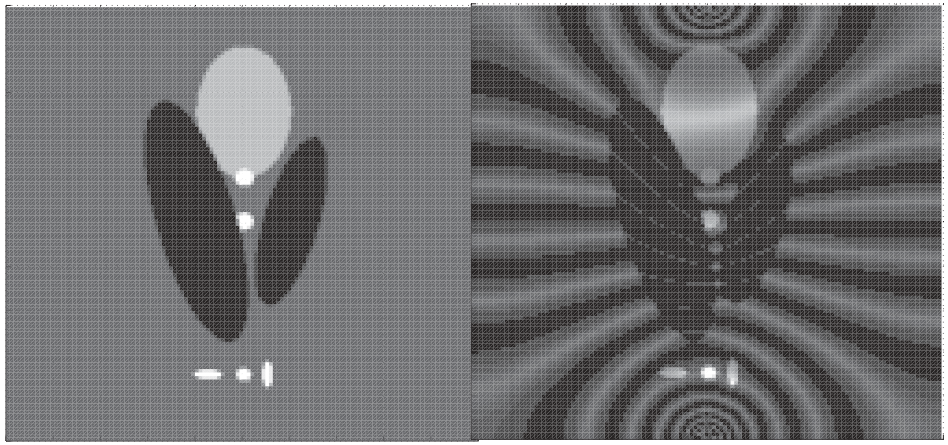

$\nabla^2 B_z$ data can trace a change of σ in the direction $\nabla u \times \hat{\mathbf{z}}$

For uniqueness, we need two linearly independent injection currents.

$$\nabla^2 B_{z,j} = \nabla \ln \sigma \cdot (\sigma \nabla u_j \times \hat{\mathbf{z}}) \qquad (j = 1, 2)$$

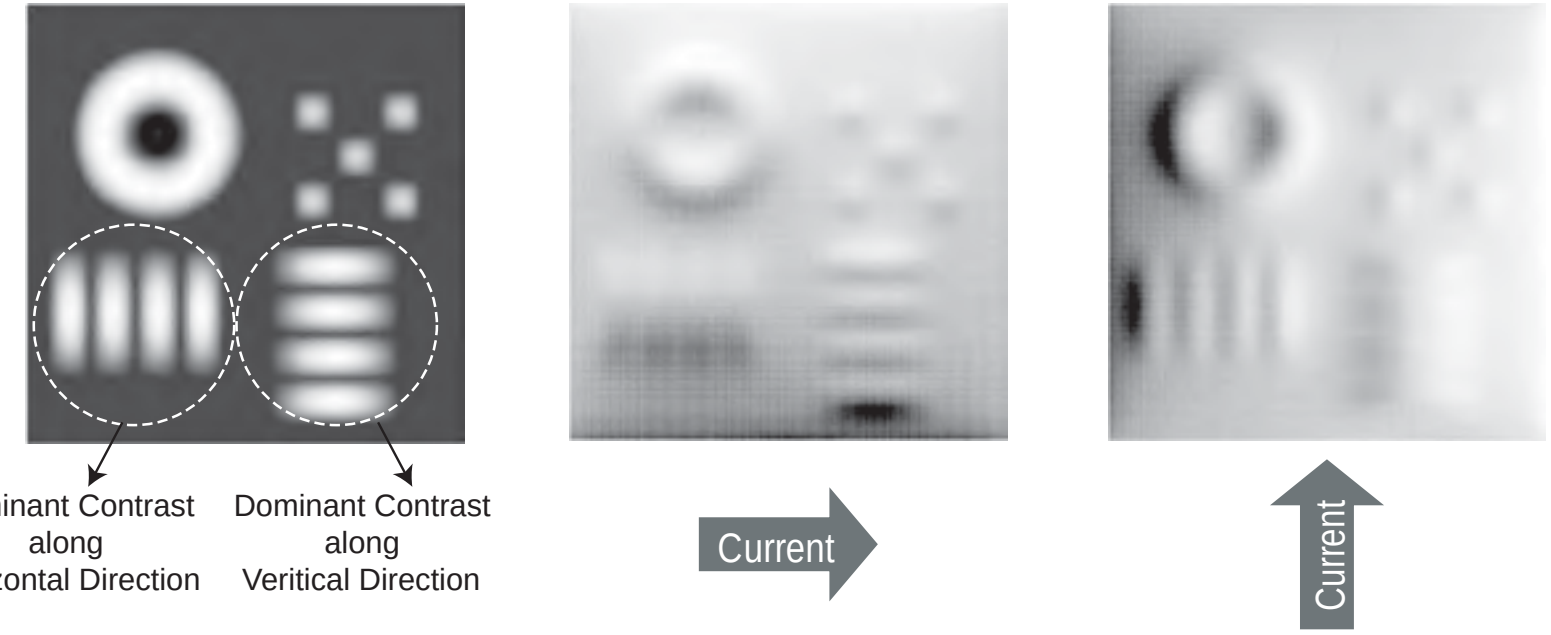

Use four electrodes to produce $B_{z,1}$ & $B_{z,2}$:

$$B_{z,j}(\mathbf{r}) = \frac{\mu_0}{4\pi} \int_\Omega \frac{\sigma(\mathbf{r}')\, \hat{\mathbf{z}} \cdot [(\mathbf{r}-\mathbf{r}') \times \nabla u_j(\mathbf{r}')]}{|\mathbf{r}-\mathbf{r}'|^3} d\mathbf{r}' \qquad (j = 1, 2)$$

where u_j satisfies

$$\begin{cases} \nabla \cdot (\sigma \nabla u_j[\sigma]) = 0 \quad \text{in } \Omega, \\ I = \int_{\mathcal{E}_j^+} \sigma \frac{\partial u_j[\sigma]}{\partial \mathbf{n}}\, ds = -\int_{\mathcal{E}_j^-} \sigma \frac{\partial u_j[\sigma]}{\partial \mathbf{n}}\, ds\,, \\ \nabla u_j[\sigma] \times \mathbf{n}|_{\mathcal{E}_j^+ \cup \mathcal{E}_j^-} = 0, \qquad \sigma \frac{\partial u_j[\sigma]}{\partial \mathbf{n}} = 0 \quad \text{on } \partial\Omega \setminus \overline{\mathcal{E}_j^+ \cup \mathcal{E}_j^-} \end{cases}$$

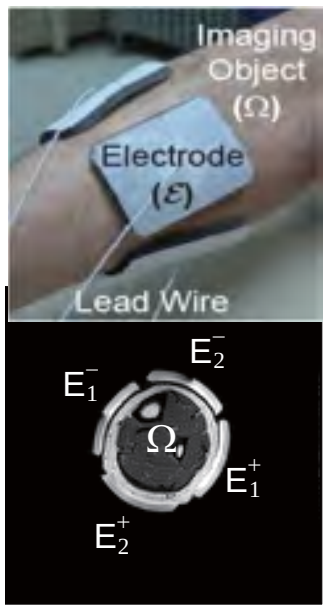

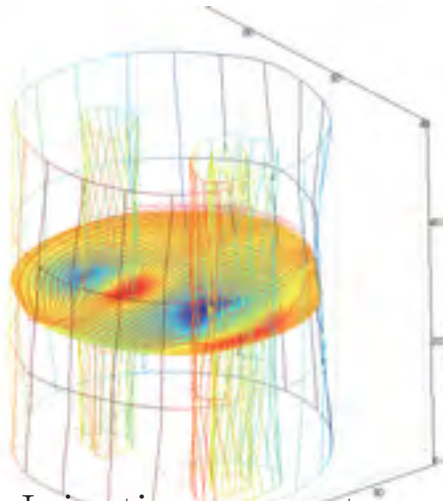

Injection current produces E, J, B

Harmonic B_z-algorithm [2002; Seo, Kwon, Yoon, Woo]

σ is reconstructed by only B_z:

$$\nabla^2_{xy} \ln \sigma = \nabla_{xy} \cdot \left(\mathbf{A}^\dagger \begin{bmatrix} \nabla^2 B_{z,1} \\ \nabla^2 B_{z,2} \end{bmatrix} \right)$$

$$\text{where} \quad \mathbf{A}^\dagger := \frac{1}{\mu_0} \begin{bmatrix} \sigma \frac{\partial u_1[\sigma]}{\partial y} & -\sigma \frac{\partial u_1[\sigma]}{\partial x} \\ \sigma \frac{\partial u_2[\sigma]}{\partial y} & -\sigma \frac{\partial u_2[\sigma]}{\partial x} \end{bmatrix}^{-1}$$

This formula exists in an implicit form owing to the nonlinear relationship between σ and B_z, but it was designed to use a fixed-point theory. The major drawback of EIT, ill-posedness is mainly due to the fact that the overall flow of $\mathbf{J}$ is insensitive to local perturbations in σ. However, the harmonic Bz method takes advantage of this fact to make the algorithm work.

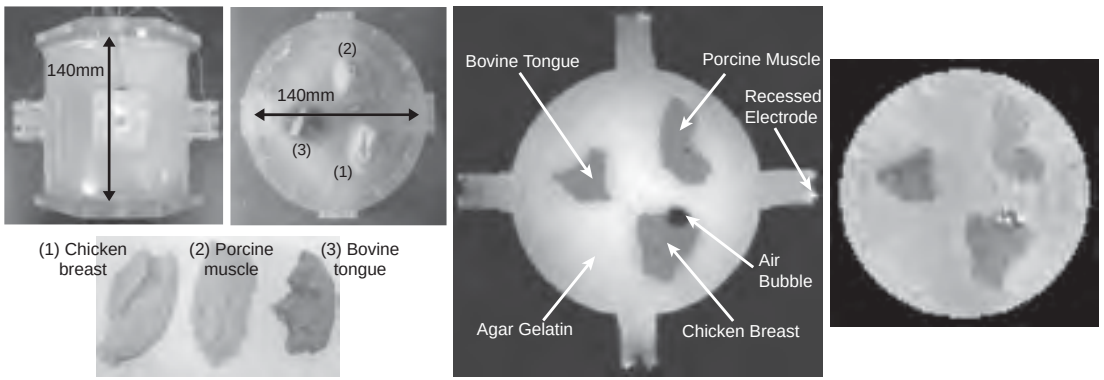

MREIT: Animal imaging experiment

Harmonic B_z-algorithm requires to solve the forward model in which we need to know Ω and Neumann data (semi-)automatically.

- **Domain Ω**: We use **segmentation methods** to extract $\partial\Omega$ from MR-image automatically.
- **Neumann boundary data**: Use semi-automatic algorithm to get Neumann condition.

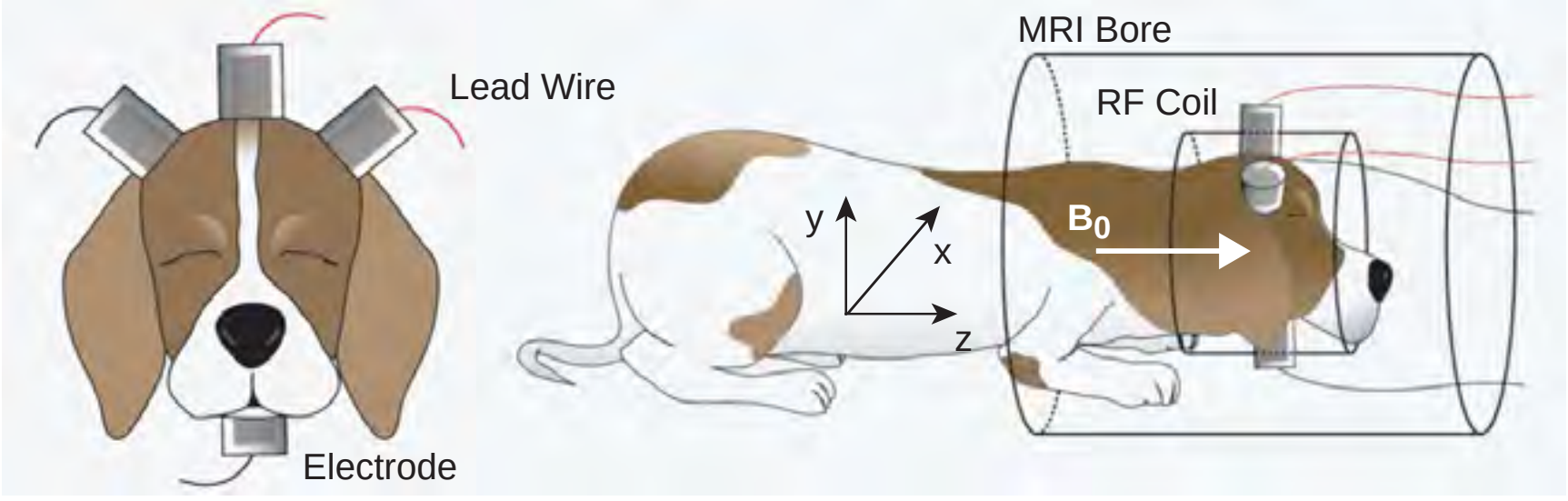

MREIT: Animal σ-imaging

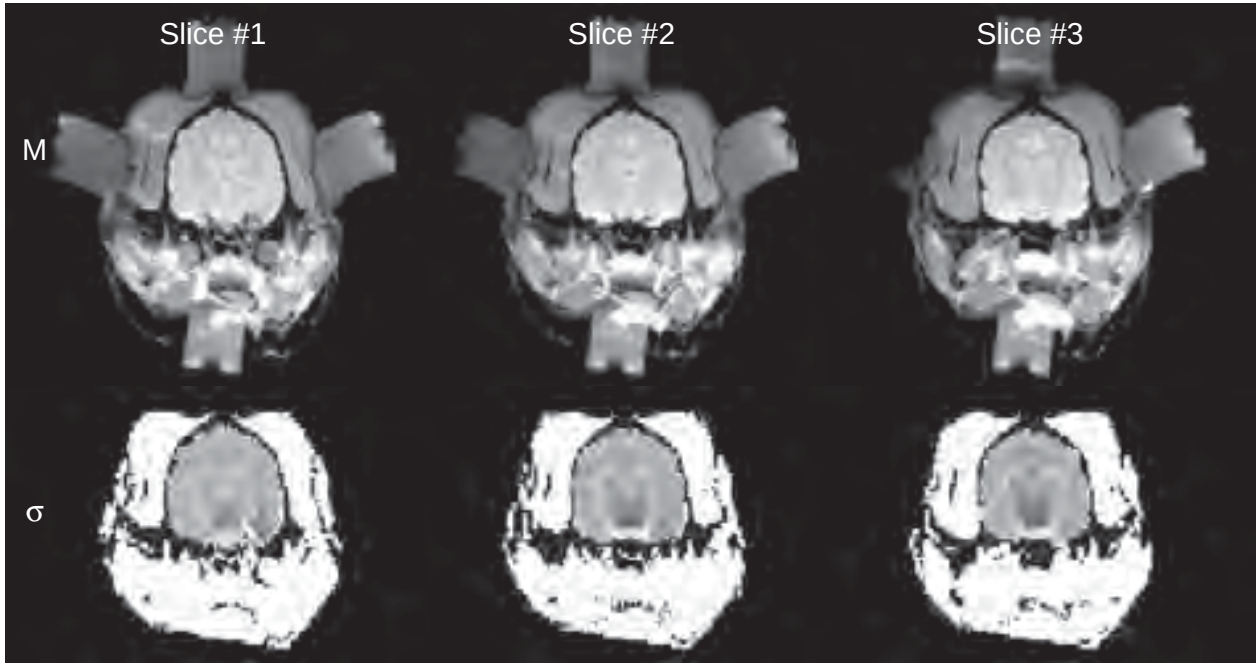

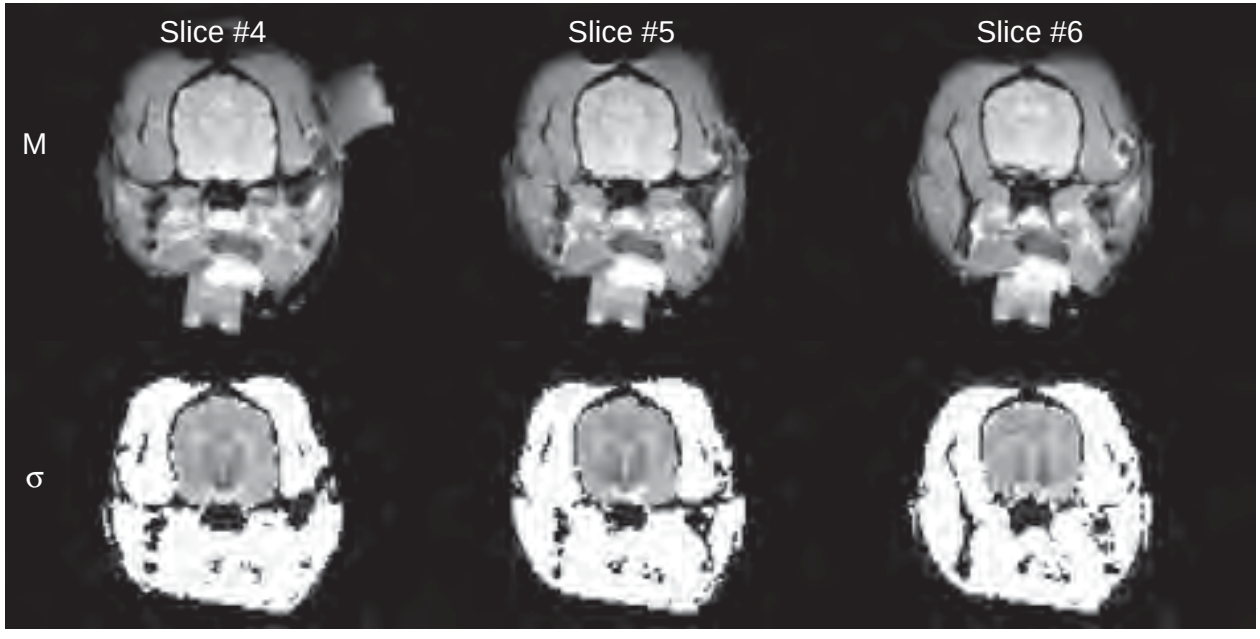

CoReHa: Software for MREIT

MREIT Matlab Toolkit(2006: CJ Park, SH Lee, Kwon, Woo, Seo), **CoReHA**(Conductivity Reconstructor using Harmonic Algorithm 2008: GW Jun, CO Lee, Woo, Seo)

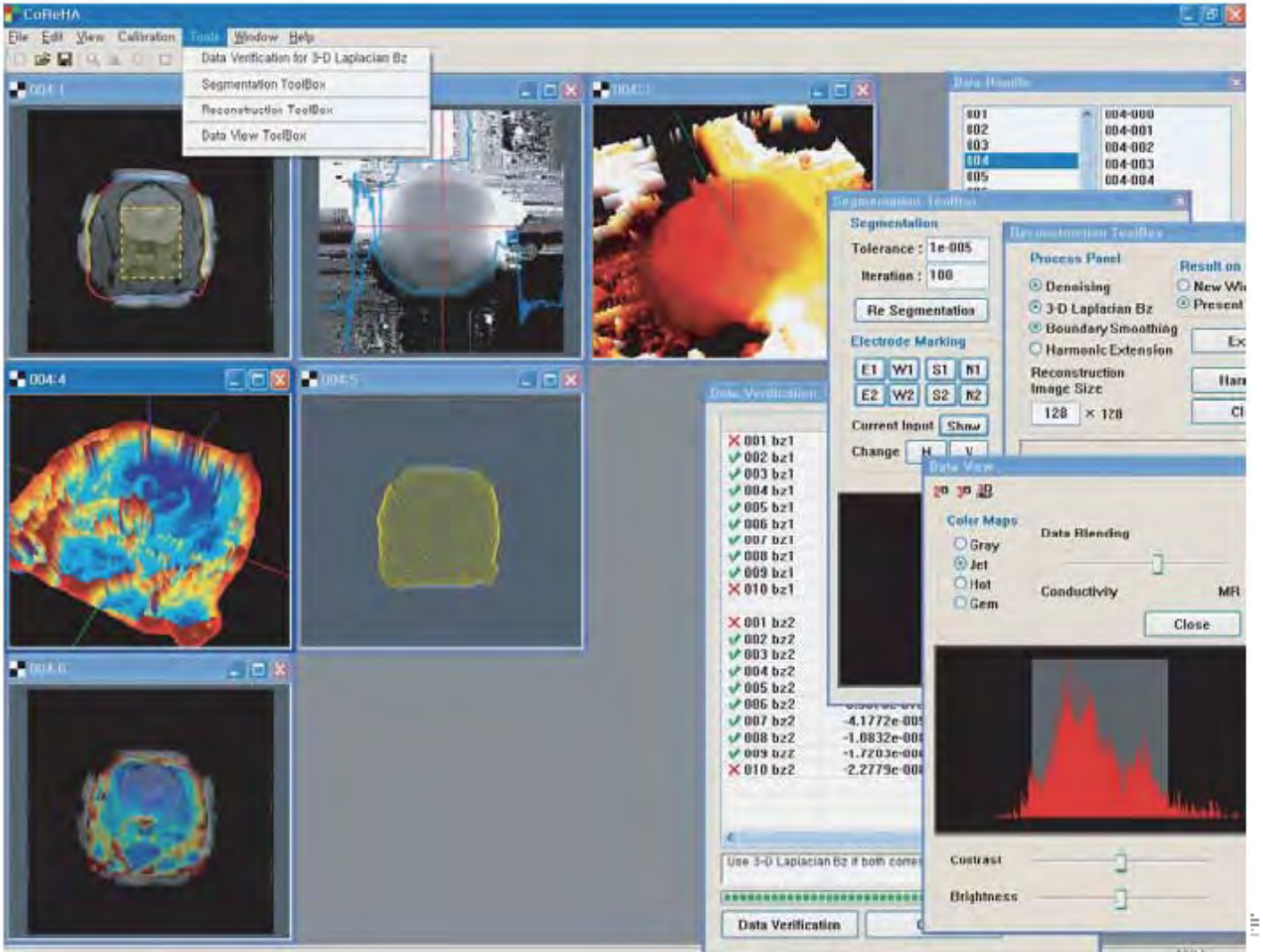

MREIT: Animal imaging

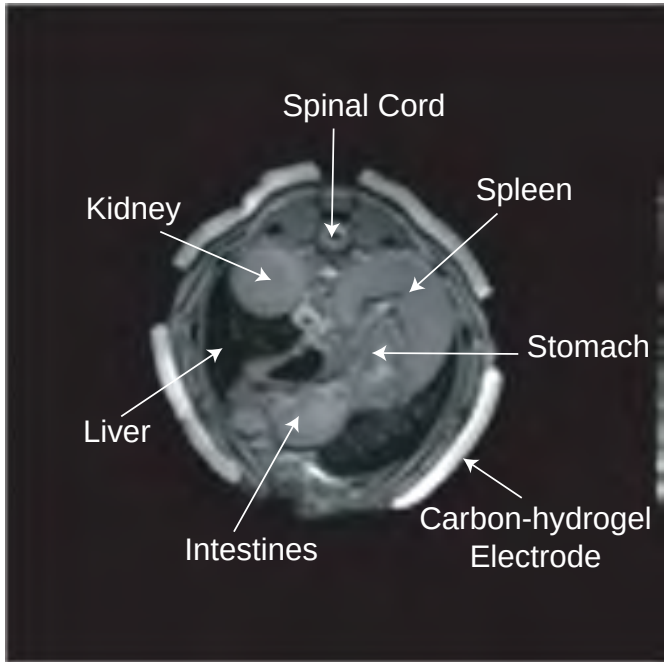

MREIT Images

MREIT is the most advanced conductivity imaging technique and now can offer state-of-the-art conductivity imaging for animal and human experiments.

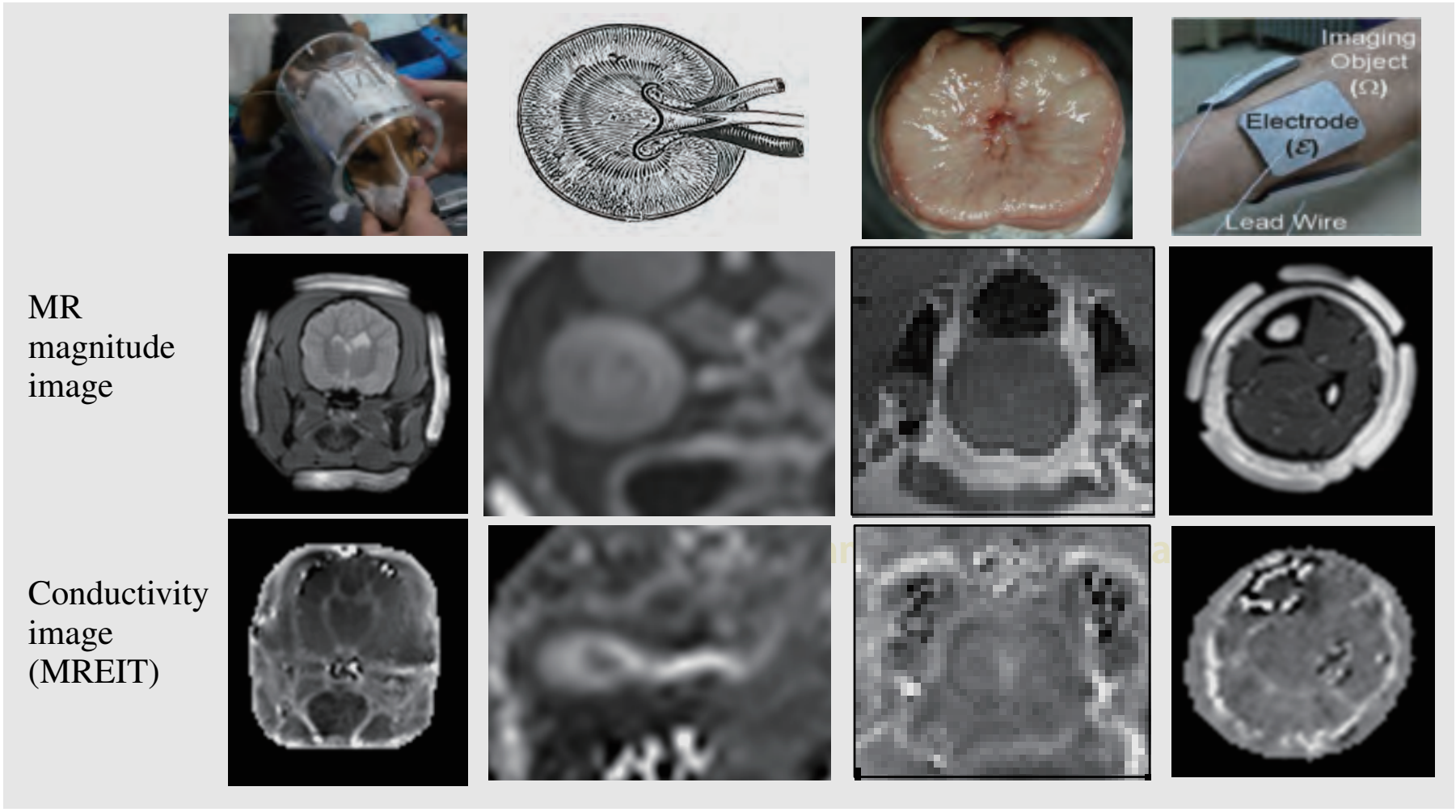

Challenging issues in year 2000: Proposal for MREIT research

- **Reconstruct conductivity using only Bz: Solved ✓**
- High resolution Image: Solved with 5mA ✓
- Anisotropic conductivity imaging: Solved mathematically but not feasible. Need fundamental studies.
- Animal Experiment: Solved ✓
- Human experiment: Partially Solved (Legs is OK but far from OK for brain.)
- Accuracy analysis: Partially Solved ✓ We made many conjectures (99.99% sure). See SIAM Review 2011 and PM (review 2008).

Challenging issue in MREIT for Human imaging.

- **FDA safety limit: 1mA**. **Reducing the amount of current $\Rightarrow$ Low SNR data $\Rightarrow$ Reconstruction errors and artifacts.** We need to handle noise.

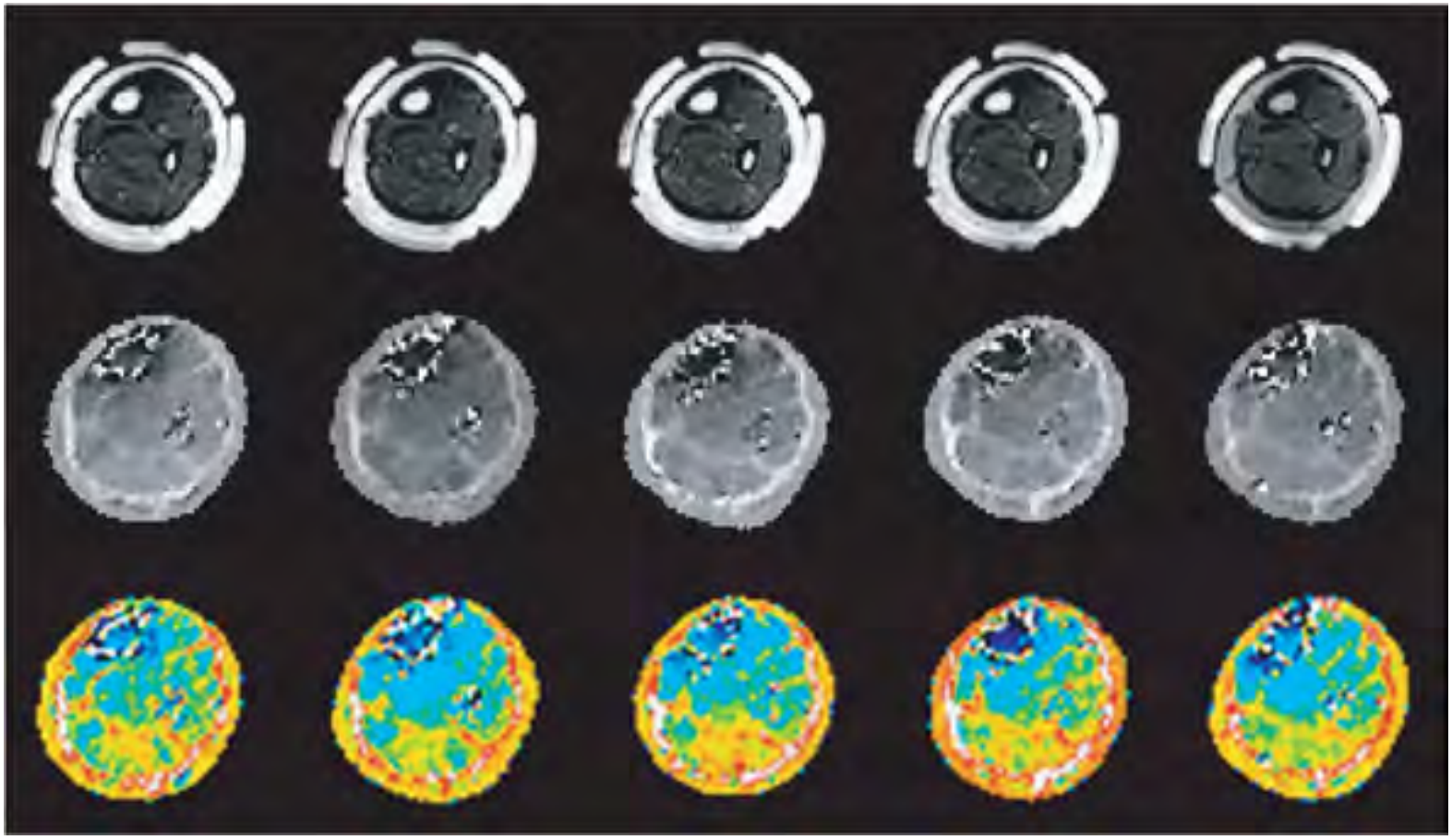

Year 2015: New Challenges in MREIT

- **High resolution Image with 1mA**
  - Low SNR: Denoising, regularization, PDE-based image restoration
  - Sensitivity enhancement by improvements in RF coil and pulse sequence
- **Functional imaging**
  - Fast imaging method: Parallel Imaging, Reduced FOV and ROI imaging
  - Sparse Sensing or Compressed Sensing (skipped K-space)
  - Statistical image analysis
- **Visual understanding effective conductivity**
- **Dual Frequency Imaging: MREIT & MREPT**

Thank you.

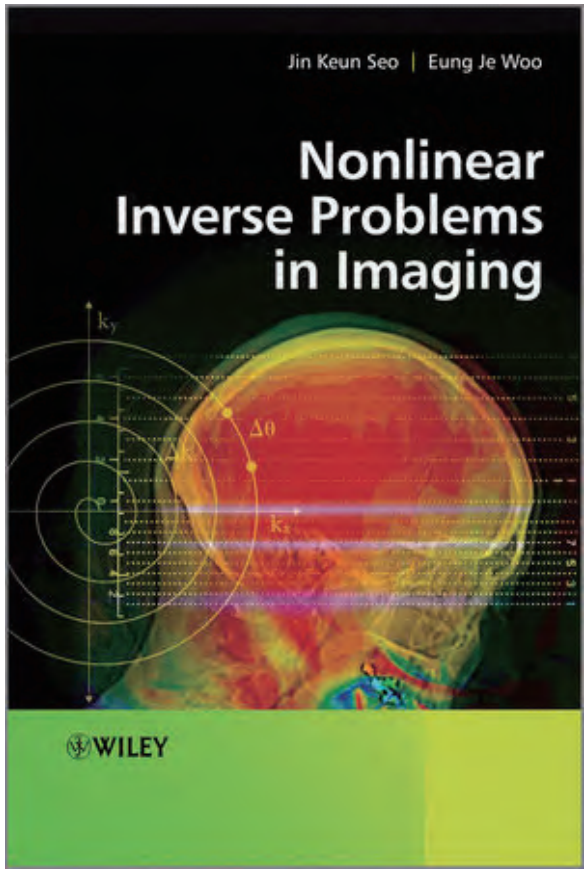

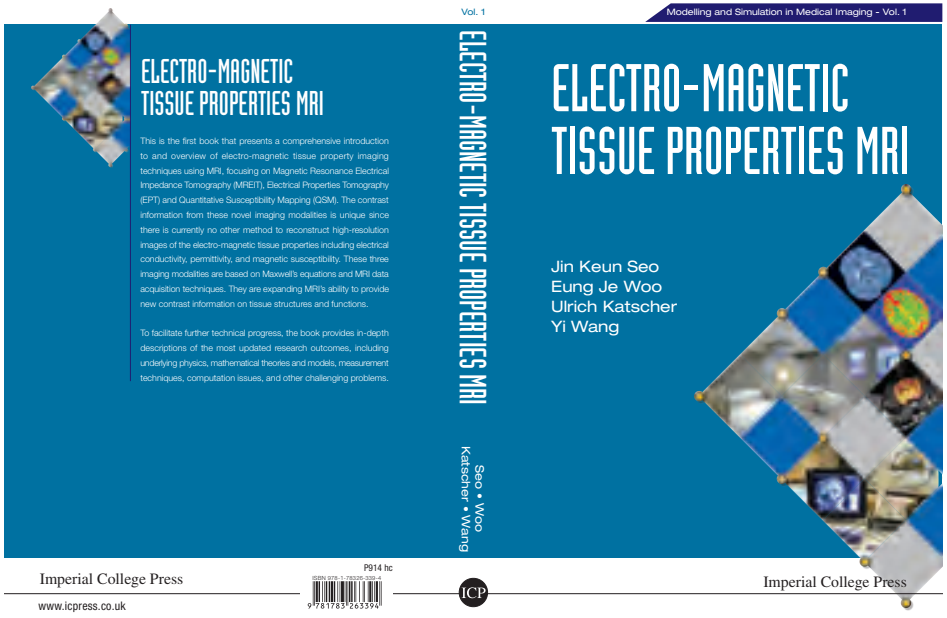

We focus on **experimental** mathematics. We develop mathematical theory in such a way that it can guide experiment on what to look for.
Modeling/Analysis⇔Numerical Simulation⇔Experiment